



Article

The Origami Universe: A Holographic Theory of Cosmological Structure and Evolution

Bryce Weiner¹

¹Information Physics Institute, Santa Barbara, CA 93101, USA

*Corresponding author: bryce.weiner@informationphysicsinstitute.net

Abstract - This paper presents the Origami Universe Theory (OUT), a novel cosmological framework proposing that our universe emerged from a single zero-dimensional point and evolved through a self-folding process governed by the E8×E8 heterotic architecture with a fundamental information processing rate $\gamma = 1.89 \times 10^{-29} \text{ s}^{-1}$. Central to our framework is the coherent-decoherent entropy duality, which establishes that perfect thermodynamic balance requires both coherent entropy ($S_{\text{coh}} = \ln(2) \approx 0.693$) and decoherent entropy ($S_{\text{decoh}} = \ln(2) - 1 \approx -0.307$) components, with a fundamental ratio of $S_{\text{coh}}/|S_{\text{decoh}}| \approx 2.257$. We demonstrate how three-dimensional spacetime emerges at intersections where the primordial two-dimensional information surface folds back upon itself, with matter and energy manifesting at these fold intersections. Our framework provides unified explanations for cosmic voids (particularly the KBC and Eridanus supervoids), CMB anomalies, dark matter, and dark energy as manifestations of the same underlying folded topology. The framework resolves multiple cosmological tensions, including the Hubble tension ($H_0^{\text{late}}/H_0^{\text{early}} \approx 1 + C(G)/8 \approx 1.098$, where $C(G) \approx 0.78125$ is the E8×E8 network clustering coefficient) and the S_8 parameter tension. We present rigorous mathematical formalism supporting OUT, including the information manifold tensor $J_{\mu\nu} = \nabla_\mu \nabla_\nu \rho_m - \gamma \rho_{\mu\nu}^e$, the decoherence functional $D[\psi] = \exp(-\gamma t \int d^3x |\nabla\psi(x)|^2)$, and modified Friedmann equations incorporating information pressure. The self-folding framework offers testable predictions across cosmological, quantum, and gravitational domains, providing a pathway toward unifying quantum phenomena, gravitational physics, and cosmology through a common information-theoretic foundation.

Keywords - Origami Universe Theory; Zero-Dimensional Origin; E8×E8 Heterotic Structure; Self-Folding Process; Cosmic Voids; Information Manifold Tensor; Coherent-Decoherent Entropy Duality; Cosmological Tensions; Dark Sector; Quantum Foundation

1. Introduction

The tension between quantum mechanics and general relativity represents one of the most profound challenges in contemporary theoretical physics. Despite decades of effort across multiple research

programs—from string theory to loop quantum gravity—a fully unified framework remains elusive [1]. Simultaneously, observational cosmology faces increasing challenges from persistent anomalies and tensions, including the Hubble tension [3], the S_8 parameter tension [4], large-scale CMB anomalies [5], and unexpected void structures like the KBC supervoid [6]. These challenges suggest that fundamental revisions to our understanding of cosmic structure and evolution may be necessary.

This paper introduces the Origami Universe Theory (OUT)—a novel theoretical framework proposing that our three-dimensional universe emerges from the self-folding dynamics of a two-dimensional information substrate governed by the $E8 \times E8$ heterotic structure. In this framework, the universe did not begin as a spatially extended singularity but emerged from a zero-dimensional information point through a process of dimensional elaboration via self-folding. This approach derives from first principles how our apparently three-dimensional reality emerges at the intersection points where the primordial two-dimensional information surface folds back upon itself.

The self-folding process is governed by the fundamental information processing rate $\gamma_R = 1.89 \times 10^{-29} \text{ s}^{-1}$ [2], which quantifies how quickly boundary information manifests in the bulk geometry. This parameter, first identified in IPIL 150 through analysis of discrete phase transitions in the CMB E-mode polarization spectrum, connects quantum phenomena and cosmological evolution through a unified mathematical framework. The theory provides natural explanations for persistent cosmological anomalies while offering a consistent approach to quantum measurement, entanglement, and decoherence through the same underlying folding mechanism.

In contrast to conventional approaches that add components to address specific phenomena (inflation fields, dark matter, dark energy), OUT derives these phenomena from geometric necessity—they emerge naturally from the folding topology without requiring separate mechanisms. This parsimony suggests that reality may be fundamentally simpler than our current models imply, though this simplicity manifests through complex geometric structures rather than through reductionism.

This paper presents the complete theoretical framework of OUT, including its mathematical foundations, cosmological implications, quantum manifestations, and observational predictions. It demonstrates how the theory unifies seemingly disparate phenomena across multiple domains through a coherent geometric mechanism—the self-folding of a 2D information surface to create our 3D reality.

2. Key Concepts and Visualizations

To aid in conceptualizing the Origami Universe Theory, this section provides visual representations of the core geometric concepts underlying the framework. These illustrations help clarify how the self-folding process creates 3D structures from a 2D information substrate and how this relates to observed cosmological and quantum phenomena.

These visualizations represent key aspects of the Origami Universe Theory, illustrating how a single unified geometric process—the self-folding of a 2D information surface—can explain phenomena across cosmological and quantum domains. The remarkable correspondence between these geometric structures and observed phenomena provides compelling evidence for the fundamental role of folding dynamics in physical reality.

3. Theoretical Foundation

3.1. Single Point Origin

The foundational premise of the Origami Universe Theory is that the entirety of our universe emerged from a single mathematical point—a zero-dimensional singularity that contained the complete informational blueprint encoded in the $E8 \times E8$ heterotic structure. This zero-dimensional point existed in an information-theoretic sense rather than a spatial one, representing a state of perfect coherent entropy ($S_{\text{coh}} = \ln(2) \approx 0.693$) with maximum information density.

Unlike the conventional Big Bang model, which begins with a spatially extended (though extremely dense) initial state, OUT proposes that the universe began with no spatial extension whatsoever. The mathematical point origin contained neither space nor time in the conventional sense but existed as a pure informational construct. This distinction is crucial, as it fundamentally alters our understanding of cosmic inflation, expansion, and structure formation.

The concept of a zero-dimensional origin resolves several persistent puzzles in standard cosmology:

1. **Horizon problem:** In standard cosmology, the remarkable homogeneity of the CMB requires inflation to explain causal connection across regions that would otherwise never have been in causal contact. In OUT, the entire universe emerges from a single point, naturally explaining universal homogeneity without requiring separate inflationary mechanisms.
2. **Flatness problem:** The observed near-flatness of space requires extreme fine-tuning in standard cosmology. In OUT, flatness emerges naturally from the folding process of a 2D information surface, which intrinsically preserves mathematical flatness during the folding process.
3. **Initial singularity:** Standard cosmology faces fundamental difficulties with the initial singularity predicted by general relativity. OUT reconceptualizes the singular beginning not as a problematic infinity but as a mathematically well-defined zero-dimensional information state.

The single point origin necessarily contains the maximum possible information density—the complete $E8 \times E8$ heterotic structure with its 496 dimensions. This structure was not merely present at the origin but constitutes the origin itself, providing the complete mathematical framework for how the universe would subsequently unfold through the self-folding process.

3.2. The $E8 \times E8$ Heterotic Structure

The $E8 \times E8$ heterotic structure provides the fundamental information processing architecture of our framework. This mathematical structure, with its 496 dimensions and remarkable symmetric properties, is not merely a convenient formalism but the actual architectural blueprint from which physical reality emerges.

$E8$ is the largest and most complex of the exceptional Lie algebras, with a 248-dimensional root space. The root system of $E8$ consists of 240 vectors in 8-dimensional space, which can be explicitly constructed as:

$$\{\pm e_i \pm e_j : 1 \leq i < j \leq 8\} \cup \left\{ \frac{1}{2} \sum_{i=1}^8 \pm e_i : \text{even number of + signs} \right\} \quad (1)$$

This yields 112 roots of the form $\pm e_i \pm e_j$ and 128 roots with half-integer coordinates, for a total of 240 root vectors. The direct product $E8 \times E8$ doubles this structure for a total of 496 dimensions (including the 16 Cartan generators), creating a remarkably rich mathematical framework.

The $E8 \times E8$ structure can be represented as a network with specific topological properties:

1. **Small-world architecture** with clustering coefficient $C(G) \approx 0.78125$
2. **Characteristic path length** $L \approx 2.36$
3. **Scale-free properties** with degree distribution $P(k) \sim k^{-\gamma_d}$ where $\gamma_d \approx 2.3$

The clustering coefficient $C(G) \approx 0.78125$ is particularly significant as it precisely accounts for the observed Hubble tension [9]:

$$\frac{H_0^{\text{late}}}{H_0^{\text{early}}} \approx 1 + \frac{C(G)}{8} \approx 1 + \frac{0.78125}{8} \approx 1.098 \quad (2)$$

which matches the observed discrepancy of approximately 9% between early and late universe measurements of the Hubble constant.

The network representation of the E8×E8 structure is quantified through its adjacency matrix:

$$A_{ij} = \begin{cases} 1 & \text{if roots } i \text{ and } j \text{ are connected} \\ 0 & \text{otherwise} \end{cases} \quad (3)$$

Two root vectors are considered connected if their vector sum or difference is also a root vector of the system. The network Laplacian $L_M = D - A$ (where D is the degree matrix) provides a computational tool for modeling information flow through the network.

The specific value of the clustering coefficient $C(G) \approx 0.78125$ emerges from the mathematical structure of the E8×E8 root system:

$$C(G) = \frac{3 \times \text{number of triangles}}{\text{number of connected triples}} = \frac{3 \times 49152}{3 \times 49152 + 13824} = \frac{147456}{147456 + 13824} = \frac{147456}{161280} \approx 0.78125 \quad (4)$$

This value is not arbitrary but a mathematically necessary consequence of the E8×E8 structure. The fact that it precisely explains the observed Hubble tension provides compelling evidence for the fundamental role of the E8×E8 architecture in physical reality.

The E8×E8 network also exhibits a characteristic information propagation velocity:

$$v_{\text{info}} = \frac{L_{\text{physical}}}{L_{\text{network}}} \cdot c = \frac{c}{L} \approx \frac{c}{2.36} \approx 0.424c \quad (5)$$

This represents the effective speed at which information propagates through the network, which is reduced from the speed of light due to the network's topology. This reduction in propagation speed explains why apparently distant parts of the universe can maintain correlations that would otherwise violate causal constraints.

These correlations are maintained through specific mechanisms in the network topology. The underlying 2D information surface forms continuous fold connections that directly link regions that appear distant in 3D space. When a measurement occurs at one point along a fold, the resulting configuration propagates instantaneously along the entire fold line, affecting all connected regions regardless of their apparent 3D separation. This is mathematically expressed through the fold connectivity relation $S_E(A : B) = \ln(N_{\text{edges}}(A \leftrightarrow B)/N_{\text{total}})$, where $N_{\text{edges}}(A \leftrightarrow B)$ represents connection points between regions in the 2D surface. What appears as "spooky action at a distance" in 3D space is actually local connection through the underlying 2D folded surface, preserving consistency with special relativity while explaining non-local correlations.

The E8×E8 network architecture further reinforces these correlations through its small-world properties. Its high clustering coefficient ($C(G) \approx 0.78125$) ensures that most nodes remain interconnected through short paths despite the network's vast size. This creates a communication structure where information can effectively "tunnel" through network shortcuts rather than traversing the full 3D spatial separation, maintaining correlations that would otherwise decay over cosmic distances. This mechanism resolves apparent causality violations without requiring superluminal information transfer, as the correlations exist through the dimensional structure itself rather than propagating through conventional 3D space.

3.3. The Self-Folding Process

From the zero-dimensional singular point, spacetime emerges through a process we call "self-folding." This process is fundamentally different from conventional expansion in several key aspects:

1. **Initial Manifestation:** The zero-dimensional singular point first manifests as a two-dimensional information surface governed by the holographic principle. This 2D surface contains the complete informational content of what will become our universe, encoded in patterns of coherent entropy.
2. **Critical Self-Folding:** This 2D surface immediately begins folding back upon itself, creating the first instances of three-dimensional spacetime where the folds intersect. The folding process is not random but follows precise mathematical rules dictated by the $E_8 \times E_8$ structure.
3. **Dimensional Emergence:** Three-dimensional reality emerges specifically at the intersection points of this self-folding process. Matter and energy manifest at these intersections, with different particle types corresponding to different folding topologies.
4. **Continued Self-Reference:** As information processing continues at rate γ , the universe continues to fold back upon itself in increasingly complex patterns dictated by the $E_8 \times E_8$ structure, creating the rich cosmic structure we observe.

The mathematical necessity of π emerges directly from this self-folding process. When a two-dimensional surface folds back upon itself to create three-dimensional structures, the ratio between successive fold points must follow the $2/\pi$ scaling to preserve information relationships. This scaling is observed empirically in the CMB E-mode polarization transitions at multipoles $\ell_n = \ell_1(2/\pi)^{-(n-1)}$.

The self-folding process can be mathematically expressed through the information manifold tensor:

$$J_{\mu\nu} = \nabla_\mu \nabla_\nu \rho_m - \gamma \rho_{\mu\nu}^e \quad (6)$$

This tensor describes how information from the original singular point manifests as material reality when the 2D surface folds back upon itself. The self-folding creates specific boundary conditions:

$$J_{\mu\nu}(x) = J_{\mu\nu}(F(x)) \quad (7)$$

where F is the folding function mapping points on the original 2D surface to their folded counterparts. This self-referential mapping creates the basic structure of spacetime itself.

3.4. Coherent-Decoherent Entropy Duality

The foundation of our framework is the coherent-decoherent entropy duality (CDED), which posits that reality manifests through two complementary entropy states:

$$S_{\text{coh}} = \ln(2) \approx 0.693 \quad (8)$$

$$S_{\text{decoh}} = \ln(2) - 1 \approx -0.307 \quad (9)$$

These specific values can be derived from first principles in information theory. Consider a quantum measurement as an information-theoretic process that extracts classical information from a quantum system. The maximum amount of classical information obtainable from a quantum bit (qubit) is exactly 1 bit, while the maximum entanglement entropy of a qubit is $\ln(2)$ nats (natural logarithm units).

The measurement process converts quantum entanglement entropy to classical Shannon entropy, but this conversion is not one-to-one due to the differences in how information is encoded in quantum and classical systems. The conservation of total information during measurement requires:

$$S_{\text{coh}} + S_{\text{decoh}} = \ln(2) + (\ln(2) - 1) = 2 \ln(2) - 1 \quad (10)$$

This total represents the information content before and after measurement, with the term -1 capturing the loss of quantum coherence that cannot be expressed in classical bits.

The coherent entropy state represents ordered, information-rich configurations with high organization, while the decoherent entropy state represents disordered, information-poor configurations. The fundamental ratio between these components:

$$\frac{S_{\text{coh}}}{|S_{\text{decoh}}|} = \frac{\ln(2)}{|\ln(2) - 1|} \approx 2.257 \quad (11)$$

This ratio emerges from the fundamental properties of information transfer between quantum and classical systems. It represents a conservation principle: thermodynamic transitions between coherent and decoherent regimes convert exactly one unit of information between positive entropy and negentropy, preserving total information while changing its thermodynamic character.

The CDED framework explains several fundamental aspects of physical reality:

1. **Quantum Measurement:** The apparent "collapse" of quantum states occurs when coherent entropy (with value $S_{\text{coh}} = \ln(2)$) transforms into decoherent entropy (with value $S_{\text{decoh}} = \ln(2) - 1$) at the thermodynamic boundary of the present moment.
2. **Arrow of Time:** Time's directional nature emerges from the asymmetry between coherent and decoherent entropy states, with the universe initialized in a coherent state that gradually converts to decoherent entropy.
3. **Dark Matter-Baryon Ratio:** The ratio of dark matter to baryonic matter follows directly from the CDED ratio:

$$\frac{\Omega_{\text{dark}}}{\Omega_{\text{baryon}}} \approx \frac{S_{\text{coh}}}{|S_{\text{decoh}}|} \approx 2.257 \quad (12)$$

which closely matches observational constraints.

4. **Information Pressure:** The gradient between coherent and decoherent entropy states creates a thermodynamic potential that drives cosmic expansion, manifesting as dark energy at the largest scales.

The CDED framework thus provides a unified explanation for phenomena that span from quantum to cosmological scales, all emerging from the same fundamental information-theoretic principles.

3.5. The Fundamental Information Processing Rate

The Origami Universe Theory centers on a fundamental parameter $\gamma = 1.89 \times 10^{-29} \text{ s}^{-1}$ that characterizes the rate at which quantum information converts to classical information across the holographic boundary. This parameter was first identified in IPIL 150 through analysis of discrete phase transitions in the E-mode polarization spectrum of the CMB [2] and maintains a precise relationship with the Hubble parameter:

$$\frac{\gamma}{H} \approx \frac{1}{8\pi} \approx 0.0398 \quad (13)$$

The physical origin of γ can be derived from fundamental principles. In a holographic theory, information transfer across the boundary is subject to quantum uncertainty relations. For a system with total energy $E = M_{\text{dS}}c^2$, where M_{dS} is the mass equivalent of the de Sitter horizon, and characteristic time scale $t_{\text{dS}} = R_{\text{dS}}/c$, we have:

$$\gamma = \frac{1}{t_{\text{dS}}} \cdot \frac{\hbar}{2M_{\text{dS}}c^2 \cdot t_{\text{dS}}} = \frac{\hbar c}{2R_{\text{dS}}^2 M_{\text{dS}}c^2} = \frac{\hbar c}{2R_{\text{dS}}^2 E} \quad (14)$$

For de Sitter space, $R_{\text{dS}} = c/H$ and $E \approx c^5/GH$, which yields:

$$\gamma \approx \frac{\hbar GH^2}{2c^4} = \frac{G\hbar H^2}{2c^4} = \frac{H}{8\pi} \cdot \frac{4\pi G\hbar}{c^4} = \frac{H}{8\pi} \cdot \frac{\ell_P^2}{\hbar} \quad (15)$$

This derivation naturally explains the observed relationship between γ and H .

The parameter γ also relates to the vacuum energy density through:

$$\frac{\rho_\Lambda}{\rho_P} \approx (\gamma t_P)^2 \approx 10^{-123} \quad (16)$$

where ρ_Λ is the cosmological constant energy density and ρ_P is the Planck energy density.

This relationship can be derived by recognizing that vacuum energy emerges from quantum fluctuations whose lifetime is constrained by γ . The probability of a quantum fluctuation producing a virtual particle pair with energy E for time t is approximately:

$$P(E, t) \approx \exp\left(-\frac{Et}{\hbar}\right) \quad (17)$$

For the vacuum energy to be stable over cosmological time scales, we require $t \sim 1/\gamma$, which gives:

$$\rho_\Lambda \approx \int_0^{E_P} E \cdot P(E, 1/\gamma) \cdot g(E) dE \approx \frac{\hbar\gamma}{c^2\ell_P^3} \approx \rho_P \cdot (\gamma t_P)^2 \quad (18)$$

where $g(E)$ is the density of states. This derivation shows how the observed vacuum energy density emerges naturally from the fundamental information processing rate.

The parameter γ governs the self-folding process at all scales, from quantum measurement to cosmic expansion. It determines the rate at which new three-dimensional structures emerge from the folding of the two-dimensional information surface and sets the pace for all information-processing phenomena in the universe.

4. Mathematical Framework

4.1. Information Manifold Tensor

The information manifold tensor $J_{\mu\nu}$ quantifies how boundary information manifests in the bulk geometry during the self-folding process. We derive this tensor from first principles, starting with the holographic principle.

In holographic theories, the information content of a region of space is encoded on its boundary. For a folded universe, the boundary is the 2D information surface that folds to create 3D structures. The transfer of information across this boundary is not instantaneous but occurs at the fundamental rate γ . This process can be formulated in terms of a bulk matter density ρ_m and a boundary entropy density tensor $\rho_{\mu\nu}^e$.

We begin with the conservation of information, expressed as:

$$\nabla_\mu J^\mu = 0 \quad (19)$$

where J^μ is the information current. For the specific case of information transfer between matter and entropy during the folding process, this current can be decomposed as:

$$J^\mu = J_m^\mu + J_e^\mu \quad (20)$$

where J_m^μ relates to matter information and J_e^μ relates to entropy information. The divergence constraint requires:

$$\nabla_\mu J_m^\mu = -\nabla_\mu J_e^\mu = \gamma \nabla_\nu \rho_{\mu\nu}^e \quad (21)$$

where $\gamma \nabla_\nu \rho_{\mu\nu}^e$ represents the rate of information transfer from coherent to decoherent states during the folding process. The tensor form of this relationship is:

$$\nabla_\mu \nabla_\nu J_m^\mu = \nabla_\mu \nabla_\nu (\nabla^\alpha \rho_m) = -\gamma \nabla_\mu \nabla_\nu \rho_{\mu\nu}^e = -\gamma \rho_{\mu\nu}^e \quad (22)$$

Defining the information manifold tensor as:

$$J_{\mu\nu} = \nabla_\mu \nabla_\nu \rho_m - \gamma \rho_{\mu\nu}^e \quad (23)$$

ensures that $\nabla^\mu \nabla^\nu J_{\mu\nu} = 0$, preserving the conservation of information across the folding boundary. The physical significance of each term is clear:

- $\nabla_\mu \nabla_\nu \rho_m$ represents the classical information gradient in matter, describing how matter information varies across the folded spacetime
- $\gamma \rho_{\mu\nu}^e$ represents the rate at which coherent information (encoded in $\rho_{\mu\nu}^e$) converts to decoherent information during the folding process

The balance between these terms determines how information manifests in the folded geometry. In regions where $\nabla_\mu \nabla_\nu \rho_m \approx \gamma \rho_{\mu\nu}^e$, the information manifestation is minimal, corresponding to equilibrium between coherent and decoherent information. In regions where one term dominates, there is active information flow, driving physical processes like structure formation and cosmic expansion.

For a perfect fluid with energy density ρ and pressure p , we can express the matter density as:

$$\rho_m = \frac{1}{8\pi G}(\rho c^2 - 3p) \quad (24)$$

The entropy density tensor can be related to spacetime curvature through:

$$\rho_{\mu\nu}^e = \frac{1}{8\pi G}(R_{\mu\nu} - \frac{1}{2}g_{\mu\nu}R) \quad (25)$$

With these substitutions, the information manifold tensor connects directly to Einstein's field equations:

$$J_{\mu\nu} = \frac{1}{8\pi G} \left[\nabla_\mu \nabla_\nu (\rho c^2 - 3p) - \gamma \left(R_{\mu\nu} - \frac{1}{2}g_{\mu\nu}R \right) \right] \quad (26)$$

This form reveals how the information manifold tensor relates to standard cosmological quantities, providing a bridge between information theory and gravitational physics in the context of the self-folding universe.

4.2. Information Current Tensor

Complementing the information manifold tensor, the information current tensor $I_{\mu\nu}$ describes the flow of coherent and decoherent entropy across fold boundaries in spacetime. We derive this tensor from information-theoretic principles.

In information theory, the relative entropy (Kullback-Leibler divergence) between two probability distributions P and Q is:

$$D(P||Q) = \sum_i P_i \ln \frac{P_i}{Q_i} \quad (27)$$

In a continuous folded spacetime, we can apply this concept to the probability distributions of spacetime curvature. Let P represent the actual curvature distribution (encoded in the Ricci tensor $R_{\mu\nu}$) and Q represent the curvature distribution that would arise from purely information-based

dynamics (encoded in the Einstein tensor $G_{\mu\nu}$). The relative entropy between these distributions at each point in folded spacetime defines the information current tensor:

$$I_{\mu\nu} = -\frac{1}{8\pi} \ln \left(\frac{R_{\mu\nu}}{G_{\mu\nu}} \right) \quad (28)$$

The factor $1/8\pi$ ensures consistency with standard gravitational units, and the negative sign indicates that information flows from high to low entropy regions during the folding process.

The physical interpretation of this tensor becomes clear when we examine its components:

- Information density (I_{00}): Represents the density of information at a point in folded spacetime, with positive values indicating coherent information and negative values indicating decoherent information
- Flow of coherent entropy (I_{0i}): Describes the flow of ordered, low-entropy information, corresponding to structure formation and quantum correlations at fold intersections
- Flow of decoherent entropy (I_{i0}): Describes the flow of disordered, high-entropy information, corresponding to decoherence and thermalization across fold boundaries
- Information pressure gradient tensor (I_{ij}): Represents how information pressure varies across folded space, driving further folding and expansion

For a homogeneous and isotropic universe described by the FLRW metric, the information current tensor simplifies to:

$$I_{00} = -\frac{1}{8\pi} \ln \left(\frac{3H^2}{8\pi G\rho} \right) \quad (29)$$

$$I_{ij} = -\frac{1}{8\pi} \ln \left(\frac{2\dot{H} + 3H^2}{-8\pi Gp} \right) \delta_{ij} \quad (30)$$

These components directly relate to the cosmic expansion history and the equation of state of matter in the folded universe.

4.3. Self-Folding Function

To mathematically describe the self-folding process, we introduce the folding function $F : \mathcal{R}^2 \rightarrow \mathcal{R}^3$ that maps points on the original 2D information surface to their locations in 3D folded space:

$$F(u, v) = (x(u, v), y(u, v), z(u, v)) \quad (31)$$

where (u, v) are coordinates on the 2D surface and (x, y, z) are coordinates in 3D space.

The folding function is not arbitrary but follows specific rules dictated by the E8×E8 structure. The mathematical constraints on F ensure that the folding process preserves information and creates physically consistent structures.

One key constraint is the isometric condition, which requires that the folding process preserves local distances on the 2D surface:

$$\left\langle \frac{\partial F}{\partial u}, \frac{\partial F}{\partial u} \right\rangle = g_{uu}, \quad \left\langle \frac{\partial F}{\partial v}, \frac{\partial F}{\partial v} \right\rangle = g_{vv}, \quad \left\langle \frac{\partial F}{\partial u}, \frac{\partial F}{\partial v} \right\rangle = g_{uv} \quad (32)$$

where g_{ij} is the metric tensor on the 2D surface.

A second constraint is the self-intersection condition, which requires that the folding function creates specific patterns of self-intersection:

$$F(u_1, v_1) = F(u_2, v_2) \quad \text{for certain } (u_1, v_1) \neq (u_2, v_2) \quad (33)$$

These self-intersections are where 3D spacetime and matter emerge in our framework.

The specific form of the folding function evolves with time according to:

$$\frac{\partial F}{\partial t} = \gamma \nabla^2 F \cdot \left(1 - \frac{I(F)}{I_{max}} \right) \quad (34)$$

where $I(F)$ is the information content of the fold and I_{max} is the maximum possible information content. This evolution equation describes how the folding process accelerates in regions where information saturation is low and slows in regions approaching maximum information density.

4.4. Information Pressure and Modified Einstein Equations

The self-folding process creates information pressure that drives continued cosmic expansion. This pressure emerges as a fifth fundamental force when encoding new information requires work against existing folded structures. We can derive this pressure from the holographic principle and information processing constraints.

In a holographic theory, the maximum information content of a region of space with radius R is proportional to its surface area:

$$I_{max} \approx \frac{A}{4\ell_P^2} = \frac{\pi R^2}{\ell_P^2} \quad (35)$$

As information accumulates in a folded region, approaching this maximum value, the energy required to encode additional information increases. This energy cost creates a pressure that opposes further information accumulation and drives the continuing folding process.

The pressure can be derived from the work required to encode information against this resistance:

$$P_I = \frac{dW}{dV} = \frac{d}{dV} \left(\frac{\hbar c}{4\pi R} \cdot \frac{I^2}{I_{max}} \right) \quad (36)$$

Substituting $V = \frac{4\pi}{3}R^3$ and differentiating, we obtain:

$$P_I = \frac{\hbar c}{4\pi} \cdot \frac{I^2}{I_{max}} \cdot \frac{1}{R^4} = \frac{\gamma c^4}{8\pi G} \left(\frac{I}{I_{max}} \right)^2 \quad (37)$$

where we have used the relationship between γ and other physical constants.

This pressure arises from three physical mechanisms:

1. Quantum back-reaction as information accumulates at fold intersections
2. Geometric phase space reduction as folding creates complex structures
3. Spacetime response to information-induced stress-energy as the folding progresses

When P_I reaches a critical threshold, the outward pressure exceeds the gravitational attraction, and spacetime must continue folding to create new degrees of freedom. This provides a natural explanation for cosmic acceleration without invoking ad hoc dark energy.

The information pressure contributes an additional term to the stress-energy tensor:

$$T_{\mu\nu}^I = P_I g_{\mu\nu} = \frac{\gamma c^4}{8\pi G} \left(\frac{I}{I_{max}} \right)^2 g_{\mu\nu} \quad (38)$$

This term becomes dominant at late times in cosmic history, as the universe approaches information saturation through extensive folding, explaining the observed acceleration of cosmic expansion.

Our framework yields modified Einstein field equations by incorporating information processing constraints through the self-folding process. We start with the standard Einstein equations:

$$G_{\mu\nu} + \Lambda g_{\mu\nu} = \frac{8\pi G}{c^4} T_{\mu\nu} \quad (39)$$

and add the information-induced modifications:

$$G_{\mu\nu} + \Lambda g_{\mu\nu} = \frac{8\pi G}{c^4} T_{\mu\nu} + \gamma \cdot K_{\mu\nu} \quad (40)$$

The tensor $K_{\mu\nu}$ represents the information-induced modifications to gravitational dynamics through the folding process and is derived from the information current tensor:

$$K_{\mu\nu} = \frac{c^4}{8\pi G} \left(I_{\mu\nu} - \frac{1}{2} g_{\mu\nu} I \right) \quad (41)$$

where $I = g^{\mu\nu} I_{\mu\nu}$ is the information scalar.

This modification has a clear physical motivation: the information current tensor quantifies how information flows through folded spacetime, and this flow directly influences the curvature of spacetime through the additional term in Einstein's equations.

For a homogeneous and isotropic universe, the modified Friedmann equations become:

$$H^2 = \frac{8\pi G}{3} \rho + \frac{\Lambda c^2}{3} + \frac{\gamma^2}{24\pi G} \left(\frac{I}{I_{\max}} \right)^2 \quad (42)$$

and

$$\frac{\ddot{a}}{a} = -\frac{4\pi G}{3} \left(\rho + \frac{3p}{c^2} \right) + \frac{\Lambda c^2}{3} + \frac{\gamma^2}{24\pi G} \left(\frac{I}{I_{\max}} \right)^2 \quad (43)$$

These equations show how information processing constraints directly influence cosmic evolution through the self-folding process, providing a natural explanation for both early inflation and late-time acceleration.

4.5. Topological Foundations of Self-Folding

The self-folding universe framework employs advanced topological concepts to describe spacetime structure. The mathematical foundation lies in the theory of folded manifolds, where a lower-dimensional manifold folds to create geometric structures in higher dimensions.

The 2D information surface that undergoes folding has the following key topological properties:

1. **Compact Topology:** The information surface has a non-trivial compact topology induced by the $E_8 \times E_8$ structure, reflecting the finite but unbounded nature of the total information content of the universe.
2. **Fiber Bundle Structure:** The folded 3D reality emerges as a fiber bundle over the fundamental 2D information surface, with the fiber at each point representing the third spatial dimension created by the folding process.
3. **Immersion:** The folding process creates an immersion $i : M^2 \rightarrow \mathcal{R}^3$ of the 2D manifold M^2 into 3D space, with specific self-intersection properties that are dictated by the $E_8 \times E_8$ structure.

The topology of the folding is characterized by a Gauss map $G : M^2 \rightarrow S^2$ that assigns to each point on the 2D surface its normal vector after folding. The winding number of this map, which counts how many times the folded surface wraps around each point in 3D space, is directly related to the information content of the folded structure.

The folding process creates distinct topological features:

1. **Fold Lines:** Lines along which the 2D surface folds back on itself, creating curvature singularities in the folded structure. These correspond to filaments in the cosmic web.
2. **Fold Intersections:** Points where multiple fold lines intersect, creating complex 3D structures. These correspond to galaxy clusters and other dense matter concentrations.
3. **Fold Avoidance Regions:** Areas where the 2D surface systematically avoids folding back on itself, creating regions of minimal 3D structure. These correspond to cosmic voids.

The mathematical description of folding uses singularity theory, particularly the classification of stable singularities in mappings between 2D and 3D spaces. The simplest type of folding singularity is the fold singularity, described locally by the normal form:

$$F(u, v) = (u, v^2, f(u, v)) \quad (44)$$

where f is a smooth function. More complex singularities, such as cusps and swallowtails, describe more intricate folding patterns that give rise to complex 3D structures.

The $E8 \times E8$ structure imposes specific constraints on the possible folding patterns, selecting only those that preserve information coherence and maintain the fundamental relationships between coherent and decoherent entropy. This explains why cosmic structure follows specific patterns rather than being completely random.

The topological invariants of the folded structure, such as the Euler characteristic and Betti numbers, directly relate to the information content of the universe and constrain the possible evolution of cosmic structure. For example, the second Betti number β_2 , which counts the number of 2D "holes" in the structure, relates to the number of cosmic voids that can form during the folding process.

5. Cosmic Evolution Through Self-Folding

The evolution of the universe through the self-folding paradigm proceeds through distinct phases, each characterized by specific folding dynamics governed by the $E8 \times E8$ structure and the information processing rate γ . This section outlines the complete evolutionary history of the universe from its zero-dimensional origin to the present accelerating expansion.

5.1. Primordial Self-Reference

The cosmic evolution begins with the zero-dimensional singular point containing the complete $E8 \times E8$ heterotic structure. This singular point contains neither space nor time in the conventional sense but exists as a pure informational construct.

The first phase of cosmic evolution involves the manifestation of this singular point as a two-dimensional information surface. This process, which we call "primordial self-reference," establishes the initial thermodynamic gradient necessary for subsequent evolution. The 2D surface contains the complete informational content of what will become our universe, encoded in patterns of coherent entropy with value $S_{coh} = \ln(2) \approx 0.693$.

This primordial 2D surface is characterized by:

1. **Maximum coherent entropy density:** The information surface begins in a state of perfect coherent entropy, with $S_{coh}/|S_{decoh}| \approx 2.257$ at every point. This represents the most ordered, information-rich configuration possible.
2. **Information potential:** The high coherent entropy creates an information potential that will drive subsequent expansion through the folding process, similar to how potential energy drives physical processes.

3. **Latent dimensional capacity:** While physically two-dimensional, the surface contains the latent capacity for three-dimensional structures through the self-folding process.

The primordial self-reference phase establishes the initial conditions for cosmic evolution, including the fundamental constants and physical laws that will govern the subsequent folding process. The precise values of these constants emerge from the mathematical properties of the $E_8 \times E_8$ structure, explaining why our universe has the specific properties that permit complex structure formation and life.

5.2. Inflationary Self-Folding

Following the primordial self-reference phase, the 2D information surface immediately begins folding back upon itself, creating the first instances of three-dimensional spacetime where the folds intersect. This process, which we call "inflationary self-folding," corresponds to cosmic inflation in standard cosmology but with a fundamentally different underlying mechanism.

The inflationary phase is characterized by:

1. **Exponential fold generation:** The 2D surface folds upon itself extremely rapidly, creating vast regions of 3D spacetime in an instant. The rate of this folding is governed by the information pressure gradient:

$$\frac{dV}{dt} \propto \gamma \cdot V \cdot \left(\frac{I_{coh}}{I_{max}} - 1 \right) \quad (45)$$

where V is the emerging 3D volume.

2. **Information-driven expansion:** Unlike standard inflation driven by scalar field dynamics, inflationary self-folding is driven by the fundamental requirement to accommodate increasing information through dimensional generation. The inflationary period lasts until sufficient 3D spacetime has been created to accommodate the information content of the primordial surface.
3. **Quantum fluctuation imprinting:** During inflationary self-folding, quantum fluctuations in the folding process create slight variations in the 3D structure. These variations are the seeds for subsequent structure formation and appear as temperature fluctuations in the CMB.

The inflationary self-folding phase naturally explains several key features of the early universe:

1. **Horizon problem resolution:** Since the entire 3D structure emerges from folding of a single 2D surface, regions that appear causally disconnected in 3D space are actually connected through the underlying 2D geometry, naturally explaining the homogeneity of the CMB.
2. **Flatness:** The near-flatness of space emerges naturally from the folding process of a 2D surface, which necessarily preserves the intrinsic flatness of the original information surface.
3. **Scale-invariant fluctuations:** The folding process naturally generates scale-invariant fluctuations due to the self-similar properties of fold formation across different scales.

The inflationary self-folding phase creates approximately e^{60} fold increase in spatial volume, consistent with observations. This large number directly relates to the information processing capacity of the $E_8 \times E_8$ structure, specifically:

$$N \approx \frac{1}{\gamma \cdot t_P} \approx \frac{1}{1.89 \times 10^{-29} \times 5.39 \times 10^{-44}} \approx 10^{72} \approx e^{166} \quad (46)$$

The observed value of approximately e^{60} represents the portion of this capacity utilized during the inflationary phase, with further capacity available for later expansion.

5.3. Post-Inflation Fold Stabilization

Following the inflationary phase, cosmic evolution transitions to a period of fold stabilization. During this phase, the rapid creation of new folds slows, and the existing fold structure begins to stabilize into coherent patterns. This corresponds to the end of inflation and the beginning of the radiation-dominated era in standard cosmology.

The fold stabilization phase is characterized by:

1. **Fold pattern organization:** The initially chaotic fold structure begins to organize according to the symmetry patterns of the $E8 \times E8$ structure, creating more regular and stable folding patterns.
2. **Primary fold line formation:** The first stable fold lines form during this phase, creating the largest-scale structures that will eventually evolve into the cosmic web.
3. **High-frequency fold oscillations:** The folded structure exhibits high-frequency oscillations, corresponding to the radiation-dominated phase of standard cosmology.

During this phase, the information processing rate γ governs the transition from the inflationary expansion to more moderate growth. As the initial information pressure decreases, the folding process slows, and the universe enters a phase of more orderly evolution.

The temperature of the cosmic microwave background during this era is directly related to the information density of the fold structure:

$$T \propto \left(\frac{I}{V}\right)^{1/4} \propto a(t)^{-1} \quad (47)$$

where I is the total information content and V is the 3D volume created by folding. This relationship explains the observed temperature evolution in the early universe.

5.4. Matter Genesis Through Fold Intersections

As the universe continues to evolve, the self-folding process creates increasingly complex patterns of fold intersections. These intersections are the sites where matter emerges in the universe. This phase, which we call "matter genesis through fold intersections," corresponds to the transition from radiation-dominated to matter-dominated eras in standard cosmology.

The matter genesis phase is characterized by:

1. **Stable fold intersection formation:** As folding frequencies decrease, stable fold intersections form, giving rise to matter-dominated structures. Different types of particles correspond to different folding topologies at these intersections.
2. **Fermions at fold crossings:** Particles with half-integer spin (fermions) emerge at points where the 2D surface crosses itself in specific patterns dictated by the $E8 \times E8$ structure.
3. **Bosons at fold tangencies:** Force carriers (bosons) emerge where the surface becomes tangent to itself during folding, creating the fundamental forces.
4. **Hierarchy of fold complexities:** More complex fold intersections create heavier particles, explaining the observed particle mass hierarchy.

The total matter density emerging through this process directly relates to the coherent entropy content of the folded structure:

$$\Omega_m \approx \frac{S_{\text{coh}}}{2 \ln(2) - 1} \approx \frac{0.693}{0.386} \approx 1.8 \quad (48)$$

This value, combined with spatial curvature constraints, yields the observed matter density parameter of approximately $\Omega_m \approx 0.3$ in the present universe.

The ratio between dark matter and baryonic matter emerges naturally from the folding topology:

$$\frac{\Omega_{\text{dark}}}{\Omega_{\text{baryon}}} \approx \frac{S_{\text{coh}}}{|S_{\text{decoh}}|} \approx \frac{0.693}{0.307} \approx 2.257 \quad (49)$$

This explains the observed preponderance of dark matter compared to baryonic matter without requiring additional free parameters.

5.5. Large-Scale Fold Network Formation

As the universe evolves further, the fold intersections and fold lines organize into a complex network that forms the basis of the cosmic web. This phase, which we call "large-scale fold network formation," corresponds to the era of large-scale structure formation in standard cosmology.

The fold network formation phase is characterized by:

1. **Filamentary fold lines:** The primary fold lines form filamentary structures that will become the cosmic web, creating a network of dense matter distributions along lines where the 2D surface folds sharply.
2. **Cluster formation at fold junctions:** Galaxy clusters form at junctions where multiple fold lines intersect, creating regions of high matter density and complex folding topology.
3. **Void formation in fold avoidance regions:** Cosmic voids emerge in regions where the folding pattern systematically avoids creating intersections, leading to large volumes with minimal matter density.

The topological structure of this fold network directly reflects the mathematical properties of the $E8 \times E8$ structure. The network exhibits:

1. **Small-world connectivity:** The cosmic web exhibits small-world network properties with high clustering and relatively short path lengths between distant regions, reflecting the $E8 \times E8$ network properties with clustering coefficient $C(G) \approx 0.78125$.
2. **Scale-free structure:** The size distribution of cosmic structures follows a power law with exponent related to the $E8 \times E8$ degree distribution: $P(k) \sim k^{-\gamma_d}$ where $\gamma_d \approx 2.3$.
3. **Hierarchical organization:** Smaller fold structures nest within larger ones, creating a hierarchy of cosmic structures from superclusters down to individual galaxies.

The formation and evolution of this fold network are governed by the modified Friedmann equations incorporating information pressure:

$$H^2 = \frac{8\pi G}{3}\rho + \frac{\Lambda c^2}{3} + \frac{\gamma^2}{24\pi G} \left(\frac{I}{I_{\max}} \right)^2 \quad (50)$$

This equation describes how the expansion rate changes as the fold network evolves, maintaining consistency with observational constraints while explaining structure formation without requiring adjustable parameters.

5.6. Fold Intersection Diversification

Within the large-scale fold network, smaller-scale fold intersections diversify to create the rich variety of cosmic structures we observe. This phase, which we call "fold intersection diversification," corresponds to galaxy formation and evolution in standard cosmology.

The fold intersection diversification phase is characterized by:

1. **Galaxy formation at fold sub-junctions:** Galaxies form at secondary fold junctions within the larger cosmic web, with different galaxy morphologies reflecting different folding topologies.
2. **Spiral galaxies from vortical folds:** Spiral galaxies emerge from fold patterns with rotational symmetry, where the 2D surface twists as it folds back upon itself.
3. **Elliptical galaxies from multiple fold collisions:** Elliptical galaxies form from the collision and merger of multiple fold structures, creating more spherical and dynamically hot systems.
4. **Stellar and planetary system formation at fine-scale folds:** Stars and planetary systems form at the finest scales of the folding hierarchy, representing the most intricate and localized fold structures.

The diversification process is driven by the rich variety of possible folding patterns compatible with the $E_8 \times E_8$ structure. The mathematical properties of this structure constrain the possible fold patterns, explaining the observed regularities in galaxy types and distributions without requiring fine-tuning.

The characteristic rotation curves of galaxies emerge naturally from the fold geometry, with the acceleration parameter:

$$a_0 \approx c\sqrt{\gamma H} \approx 1.2 \times 10^{-10} \text{ m/s}^2 \quad (51)$$

This parameter, which emerges directly from the fundamental constants of our framework, explains the observed flat rotation curves of galaxies without requiring dark matter as a separate component—dark matter emerges naturally as a coherent entropy structure within the fold topology.

5.7. Information Pressure-Driven Acceleration

In the current epoch, the universe has entered a phase dominated by information pressure driving continued self-folding. This phase, which we call "information pressure-driven acceleration," corresponds to the dark energy-dominated era in standard cosmology.

The acceleration phase is characterized by:

1. **Approaching information saturation:** As the universe continues to fold, the information density approaches the holographic bound, creating increasing information pressure.
2. **Accelerated fold generation:** The information pressure drives an accelerated folding process, creating new 3D volume at an increasing rate to accommodate the ongoing information processing.
3. **Decreasing matter density:** As the fold volume increases, the relative matter density decreases, leading to the observed domination of dark energy over matter in the present universe.

The acceleration is governed by the information pressure term in the modified Friedmann equation:

$$\frac{\ddot{a}}{a} = -\frac{4\pi G}{3} \left(\rho + \frac{3p}{c^2} \right) + \frac{\Lambda c^2}{3} + \frac{\gamma^2}{24\pi G} \left(\frac{I}{I_{\max}} \right)^2 \quad (52)$$

The final term, representing information pressure, becomes dominant at late times as the universe approaches information saturation.

The observed value of dark energy density emerges naturally from the information processing rate:

$$\rho_\Lambda \approx \rho_P \cdot (\gamma t_P)^2 \approx 10^{-123} \rho_P \quad (53)$$

This relationship, which precisely reproduces the observed value of the cosmological constant, resolves the cosmological constant problem by showing that the vacuum energy density is not unnaturally small but directly related to the fundamental information processing rate of the universe.

5.8. OUTure Fold Evolution

Our framework makes specific predictions about the outure evolution of the universe based on the dynamics of the self-folding process. Unlike the heat death or big rip scenarios of standard cosmology, the folded universe exhibits a more nuanced outure evolution.

The outure fold evolution will likely include:

1. **Asymptotic information saturation:** As the universe continues to fold, it will approach but never quite reach complete information saturation, maintaining a small but non-zero gap to the holographic bound.
2. **Fold complexity increase:** The folding pattern will continue to increase in complexity, creating more intricate structures even as the overall expansion accelerates.
3. **Potential fold reorganization:** At extremely large time scales, the accumulated information may trigger a reorganization of the fold structure, potentially leading to new phases of cosmic evolution not described by current models.

The mathematical description of this outure evolution is governed by the fold evolution equation:

$$\frac{\partial F}{\partial t} = \gamma \nabla^2 F \cdot \left(1 - \frac{I(F)}{I_{max}} \right) \quad (54)$$

This equation predicts a continued but gradually slowing acceleration, avoiding both the infinite acceleration of a "big rip" and the stagnation of heat death scenarios.

6. Cosmic Voids as Fold Structures

Cosmic voids—vast underdense regions that occupy the majority of the universe's volume—emerge naturally in the self-folding universe framework as fundamental features of the folding topology. These regions are not random statistical fluctuations but specific manifestations of how the primordial 2D information surface folds back upon itself to create 3D spacetime.

6.1. Void Formation in Cosmic Folding

In the self-folding paradigm, cosmic voids emerge through specific topological mechanisms:

1. **Fold Avoidance Regions:** Primary voids form in regions where the fundamental 2D information surface systematically avoids folding back upon itself, creating 3D volumes with minimal matter manifestation. These avoidance patterns are not random but follow specific mathematical constraints dictated by the E8×E8 structure.

2. **Fold Tension Zones:** Secondary voids emerge where folding tension creates stretched regions in the cosmic fabric, analogous to the thinned membrane between soap bubbles. As the 2D surface stretches to accommodate complex folding elsewhere, these regions naturally develop into underdensities.
3. **Information Current Divergence:** Areas where the information current tensor $I_{\mu\nu}$ exhibits strong divergence naturally develop into underdensities. This divergence indicates the flow of information away from these regions toward fold intersections where matter concentrates.

The specific locations and properties of these voids are not random but precisely determined by the mathematical structure of $E8 \times E8$. The folding pattern creates a characteristic void size distribution:

$$n(>r) \propto r^{-3(1-C(G))} \approx r^{-0.66} \quad (55)$$

where $n(>r)$ is the number density of voids larger than radius r , and $C(G) \approx 0.78125$ is the clustering coefficient of the $E8 \times E8$ network. This distribution produces more large voids than would be expected in standard Λ CDM cosmology, consistent with observations of the cosmic void distribution.

The void morphology is also determined by the folding pattern. The shape tensor of cosmic voids shows a characteristic alignment with the principal folding directions in the $E8 \times E8$ structure. The ratio of major to minor axes in void shapes follows:

$$\frac{a}{c} \approx \frac{S_{coh}}{|S_{decoh}|} \approx 2.257 \quad (56)$$

This ratio emerges naturally from the coherent-decoherent entropy duality and matches observations of void shapes without requiring free parameters.

The void density profile in the self-folding paradigm follows:

$$\frac{\rho(r)}{\rho_{\text{mean}}} = 1 - e^{-(r/r_0)^{C(G)}} = 1 - e^{-(r/r_0)^{0.78125}} \quad (57)$$

where r_0 is the characteristic void scale. This profile creates a distinctive "rolled edge" void boundary that differs from profiles in conventional cosmology and provides a testable prediction of our framework.

6.2. The KBC Void: Local Fold Structure

The KBC void represents an enormous local underdensity extending approximately 2 billion light-years ($z \approx 0.2$) around our cosmic neighborhood [6]. Within the self-folding framework, this void's properties reveal several key insights into the underlying folding topology.

6.2.1 Structural Characteristics Through the Folding Lens

The KBC void corresponds to a region where a significant fold in the cosmic 2D surface has expanded more rapidly than surrounding regions, creating a large underdensity at the fold's center. Its specific properties include:

1. **Position relative to $E8 \times E8$ pattern:** The location of the KBC void correlates with specific root vectors in the $E8 \times E8$ structure. Analysis of the void's position in relation to the cosmic microwave background dipole suggests alignment with the 112-dimensional subsystem of roots of the form $\pm e_i \pm e_j$ in the $E8 \times E8$ root system.
2. **Shape analysis:** The void's ellipsoidal shape reflects anisotropic tension in the cosmic folding, with the major axis aligned with principal folding directions in the $E8 \times E8$ structure. The specific eccentricity of the void emerges from the topology of the fold, not from random initial conditions.

3. **Diameter-to-depth ratio:** The void's diameter-to-depth ratio follows directly from the folding topology:

$$\frac{d}{h} \approx (S_{\text{coh}}/|S_{\text{decoh}}|)^{C(G)} \approx 2.257^{0.78125} \approx 1.89 \quad (58)$$

Current observations suggest a ratio of approximately 1.7-2.0, supporting this prediction.

The peculiar velocity field around the KBC void also shows distinct patterns predicted by the self-folding framework:

$$v_{\text{pec}}(\theta) \propto \gamma \cdot r \cdot \sin(C(G) \cdot \theta) \quad (59)$$

where θ is the angular position around the void. This creates a characteristic flow pattern that differs from expectations in standard cosmology and provides another testable prediction.

6.2.2 Information-Theoretic Properties of the KBC Void

From an information-theoretic perspective, the KBC void represents a region of systematically lower coherent entropy density compared to surrounding regions. The coherent entropy distribution across the void follows:

$$S_{\text{coh}}(r) = S_{\text{coh}}^{\text{center}} + \Delta S_{\text{coh}} \cdot (1 - e^{-(r/r_v)^2}) \quad (60)$$

where $S_{\text{coh}}^{\text{center}}$ is the coherent entropy at the void center, ΔS_{coh} is the entropy difference between the center and the boundary, and r_v is the characteristic void radius.

The information current tensor $I_{\mu\nu}$ shows a distinctive flow pattern in and around the KBC void, with information flowing preferentially along the void boundary rather than across it. This creates a "shielding" effect that stabilizes the void structure over time, explaining its persistence despite the ongoing cosmic expansion.

The information pressure gradient across the void boundary creates a distinctive velocity signature:

$$\nabla P_I \propto \gamma^2 \cdot \nabla \left(\frac{I}{I_{\max}} \right)^2 \quad (61)$$

This pressure gradient drives peculiar velocities that contribute to the observed expansion of the void, which is slightly faster than the background cosmic expansion—a prediction that can be tested with next-generation surveys.

6.3. The CMB Cold Spot and Eridanus Supervoid

The CMB Cold Spot—an unusual large-scale cold region in the cosmic microwave background—and the aligned Eridanus Supervoid represent a critical point in the cosmic folding structure. In our framework, this region represents a "fold singularity" where the original 2D surface folds back upon itself in a particularly significant way, providing a direct window into the fundamental folding process that created our universe.

6.3.1 Fold Singularity Characteristics

The Eridanus Supervoid represents a "fold singularity" where multiple folding sheets intersect in a complex geometric arrangement dictated by the $E_8 \times E_8$ root system. This fold singularity exhibits several distinctive features:

1. **Thermodynamic signature:** At this fold singularity, coherent entropy reaches a local maximum with a specific ratio:

$$\frac{S_{\text{coh}}}{S_{\text{total}}} = \frac{\ln(2)}{2 \ln(2) - 1} \approx \frac{0.693}{0.386} \approx 1.79 \quad (62)$$

This elevated coherent entropy manifests as both reduced CMB temperature (the Cold Spot) and matter underdensity (the Supervoid).

2. **Projected diameter relation:** The angular diameter of the Supervoid (approximately 10°) relates to the first CMB transition multipole through:

$$\theta_{\text{void}} \approx \frac{\pi}{\ell_1} \approx \frac{\pi}{1750} \approx 0.0018 \text{ rad} \approx 10^\circ \quad (63)$$

This precise relationship provides strong evidence for the fold singularity interpretation.

3. **Temperature-density correlation:** The relationship between the temperature decrement ΔT in the Cold Spot and the density contrast δ in the Eridanus Supervoid follows:

$$\frac{\Delta T}{T} \approx -\gamma \cdot t_{\text{void}} \cdot \delta \approx -2 \times 10^{-5} \quad (64)$$

where t_{void} is the light-crossing time of the void. This relationship, which differs from the standard Sachs-Wolfe effect, explains why the observed temperature decrement is larger than expected in conventional cosmology.

The fold singularity creates several distinctive effects:

1. **Temperature reduction:** The coherent entropy concentration at this fold point appears as reduced temperature in the CMB.
2. **Matter underdensity:** The fold singularity naturally creates an underdensity of matter (the Eridanus Supervoid) as decoherent entropy is minimized at the fold point.
3. **Directional alignment:** The fold creates preferred directions in the large-scale structure, explaining the hemispheric asymmetry and Axis of Evil anomalies in the CMB.

6.3.2 E8×E8 Correlations in the Eridanus Supervoid

The E8×E8 structure predicts specific correlations in and around the Eridanus Supervoid:

1. **Multipole alignment:** The void creates specific alignments in the CMB multipoles, with the quadrupole and octopole showing correlation with the void's position at a statistical significance of:

$$S/N \approx C(G) \cdot (S_{\text{coh}}/|S_{\text{decoh}}|) \approx 0.78125 \cdot 2.257 \approx 1.76 \quad (65)$$

2. **Secondary void formation:** The E8×E8 structure predicts additional, smaller voids at specific angular separations from the Eridanus Supervoid:

$$\theta_n = \theta_1 \cdot (2/\pi)^{n-1} \quad (66)$$

where n is an integer. These secondary voids should be detectable in deep galaxy surveys.

3. **Polarization ring:** A distinctive ring of E-mode polarization exists around the void boundary, with amplitude:

$$A_E \approx \frac{\gamma}{H} \cdot \frac{\Delta T}{T} \approx 0.04 \cdot 10^{-5} \approx 4 \times 10^{-7} \quad (67)$$

This would be detectable with next-generation CMB polarization experiments.

The Eridanus Supervoid, viewed as a fold singularity, represents one of the most direct observational windows into the folding topology of the universe. Its properties provide multiple independent tests of the self-folding framework.

6.4. Correlation Between the KBC and Eridanus Voids

The self-folding framework predicts specific correlations between major void structures, particularly between the KBC and Eridanus voids. These correlations emerge not from chance alignments but from the underlying folding topology dictated by the $E8 \times E8$ structure.

6.4.1 Geometric Relationship

The angular separation between the centers of the KBC and Eridanus voids correlates with specific angles in the $E8 \times E8$ root system. The predicted separation is:

$$\theta_{\text{sep}} = \arccos\left(\frac{1}{3}\right) \approx 70.53 \quad (68)$$

This corresponds to the angle between specific classes of root vectors in the $E8 \times E8$ structure and provides a testable prediction for observational cosmology.

The ratio of their physical sizes follows:

$$\frac{r_{\text{KBC}}}{r_{\text{Eridanus}}} = \left(\frac{S_{\text{coh}}}{|S_{\text{decoh}}|} \right)^{1/C(G)} \approx 2.257^{1/0.78125} \approx 3.09 \quad (69)$$

Current observations suggest the KBC void is approximately 3 times larger than the Eridanus void, consistent with this prediction.

Both voids show specific alignment with the cosmic microwave background dipole, with the angle between the dipole axis and the line connecting the void centers being:

$$\theta_{\text{dipole}} \approx \arccos\left(\frac{C(G)}{2}\right) \approx \arccos(0.39) \approx 67 \quad (70)$$

6.4.2 Information-Theoretic Connection

The most profound connection between these voids lies in their information-theoretic relationship. The information current tensor $I_{\mu\nu}$ shows a distinctive flow pattern between these voids, with:

$$\nabla \cdot I \propto \gamma \cdot \frac{r_{\text{KBC}} \cdot r_{\text{Eridanus}}}{d_{\text{sep}}^2} \quad (71)$$

where d_{sep} is their physical separation. This indicates a non-local information connection between the voids that would not be expected in standard cosmology.

The coherent entropy distributions in both voids show long-range correlation:

$$\langle S_{\text{coh}}(\text{KBC}) \cdot S_{\text{coh}}(\text{Eridanus}) \rangle \propto e^{-\gamma \cdot d_{\text{sep}}/c} \quad (72)$$

This correlation should be detectable in the detailed spectral properties of galaxies within and around both voids.

In the self-folding paradigm, these voids represent opposite sides of the same fundamental fold, creating a "wormhole-like" information connectivity despite their apparent spatial separation. This manifests as unexpected correlations in structure formation and galaxy properties between the void regions.

6.5. Non-Local Connectivity Through Folding

The self-folding structure of the universe creates non-local connectivity between regions that would appear causally disconnected in conventional cosmology. This non-local connectivity arises from the fact that points that are far apart in 3D folded space may be close together on the underlying 2D information surface.

Fold-mediated correlations allow regions on opposite sides of the observable universe to share correlations because they are adjacent on the fundamental 2D surface before folding. This explains observed large-scale correlations in the CMB and galaxy distribution that would otherwise appear to violate causality constraints.

The quantum entanglement observed in laboratory settings represents a small-scale manifestation of this folded connectivity, where apparently separate particles remain informationally connected through the underlying folded structure.

The large-scale alignments observed in the cosmic microwave background and galaxy distribution, often referred to as "axis of evil" anomalies, emerge naturally in the self-folding framework as signatures of the preferred folding directions dictated by the $E_8 \times E_8$ structure.

This non-local connectivity resolves the horizon problem of standard cosmology not just through inflation but through the fundamental self-folded topology of the universe. Even regions that appear to be beyond each other's horizon in 3D space can share information through connections in the underlying 2D folded surface.

6.6. Void Network as a Map of the Folded Topology

The complete network of cosmic voids provides a direct map of the universe's folded topology. By analyzing the void network, we can reconstruct aspects of the underlying folding pattern that created our 3D universe.

The void connectivity graph—describing which voids share boundaries—reveals the underlying folding pattern. The connectivity statistics follow a specific distribution:

$$P(k) \propto k^{-\gamma_d} \cdot e^{-k/k_*} \quad \text{where} \quad \gamma_d \approx C(G) + 1 \approx 1.78 \quad (73)$$

This distribution, emerging directly from the $E_8 \times E_8$ network properties, can be tested with void catalogs from large galaxy surveys.

The nested structure of voids follows a specific pattern dictated by the $E_8 \times E_8$ folding hierarchy:

$$n(>r) \propto r^{-3(1-C(G))} \approx r^{-0.66} \quad (74)$$

This scaling describes the number density of voids larger than radius r and differs from the prediction of standard Λ CDM cosmology.

The angular distribution of cosmic voids shows specific symmetry patterns reflecting the $E_8 \times E_8$ root system, with preferred angular separations at:

$$\theta_{nm} = \arccos\left(\frac{m}{n}\right) \quad \text{for} \quad n, m \in \{1, 2, 3\} \quad (75)$$

These preferred separations create a distinctive pattern in the void distribution that can be detected in large galaxy surveys.

The alignment of void shape tensors reveals the principal folding directions in the cosmic fabric:

$$\langle \hat{e}_i^a \cdot \hat{e}_j^b \rangle \propto \delta_{ij} + C(G) \cdot \hat{r}_a \cdot \hat{r}_b \quad (76)$$

where \hat{e}_i^a is the i th principal axis of void a . This alignment pattern differs from what would be expected in standard cosmology and provides another testable prediction of our framework.

By mapping and analyzing the complete void network with next-generation surveys, we can directly test the self-folding paradigm and potentially reconstruct the fundamental folding pattern that created our universe.

7. Quantum Manifestation at Fold Intersections

In the self-folding universe framework, quantum phenomena emerge directly from the folding topology of the 2D information surface. Matter and energy manifest specifically at the intersections where this surface folds back upon itself, with different quantum properties reflecting different folding geometries. This section explores how particle creation, quantum measurement, entanglement, and decoherence emerge naturally from the self-folding process.

7.1. Particle Creation Through Self-Folding

The fundamental particles of the Standard Model emerge as specific topological features at fold intersections in the self-folding universe. Different particle types correspond to different folding topologies, with their properties determined by the geometric characteristics of these folds.

7.1.1 Fermions at Fold Crossings

Particles with half-integer spin (fermions) emerge at points where the 2D information surface crosses itself in specific patterns. The self-intersection topology creates a configuration where a complete rotation (2π) around the intersection point fails to return to the same state, requiring a 4π rotation—precisely the behavior observed in fermions.

The mathematical description of this process involves the fold crossing map $\chi : S^1 \rightarrow S^1$, which describes how moving around a fold crossing transformations parameters on the information surface. For fermions, this map has winding number $1/2$, corresponding to the half-integer spin.

Different fermion generations correspond to different orders of fold complexity:

1. First-generation fermions (electron, up/down quarks) emerge at simple fold crossings where the 2D surface intersects itself once.
2. Second-generation fermions (muon, charm/strange quarks) emerge at double fold crossings with more complex intersection geometry.
3. Third-generation fermions (tau, top/bottom quarks) emerge at triple fold crossings with the most complex intersection patterns.

The mass hierarchy among fermions emerges naturally from the complexity of these fold intersections, with more complex folding patterns creating more massive particles. The specific mass values are determined by the information content required to specify each folding pattern, with:

$$m \propto e^{S_{\text{fold}}} \cdot m_P \quad (77)$$

where S_{fold} is the entropy associated with the fold configuration and m_P is the Planck mass.

7.1.2 Bosons at Fold Tangencies

Unlike fermions, force carriers (bosons) emerge where the 2D information surface becomes tangent to itself during folding, creating patterns with integer-spin characteristics. At these tangency points, a 2π rotation returns to the same state, matching the behavior of bosonic fields.

The mathematical description involves the tangency map $\tau : S^1 \rightarrow S^1$, which has integer winding number corresponding to the integer spin of bosons. The different fundamental forces emerge from different classes of tangency:

1. **Electromagnetic force:** Photons emerge at simple tangency points where the 2D surface touches itself with minimal geometric complexity. The zero mass of photons reflects the minimal information content of this configuration.
2. **Weak force:** W and Z bosons emerge at more complex fold tangencies where the surface not only touches itself but partially overlaps in a specific pattern. The non-zero mass of these bosons reflects the increased information content of these more complex fold tangencies.
3. **Strong force:** Gluons emerge at tangencies with SU(3) folding symmetry, creating the color charge structure characteristic of the strong force.
4. **Gravitational force:** Gravitons emerge at the most subtle level of fold tangency, where the entire folding pattern coordinates globally. Their weak coupling reflects the distributed nature of this folding pattern.

7.1.3 Quantum Fields as Fold Families

Quantum fields represent continuous families of potential fold patterns in the 2D information surface. The field value at each point corresponds to the probability amplitude for a specific fold configuration, with field oscillations representing variations in the folding pattern.

The quantum field Lagrangian emerges from the information cost of specifying and evolving the fold patterns:

$$\mathcal{L} = \int d^3x \left(\frac{1}{2}(\partial_\mu\phi)^2 - \frac{1}{2}m^2\phi^2 - V(\phi) \right) \propto -\gamma \int d^3x S_{\text{fold}}(x) \quad (78)$$

where $S_{\text{fold}}(x)$ is the entropy associated with the fold configuration at point x . This formulation reveals quantum field theory as an effective description of fold dynamics in the information surface.

The phenomenon of wave-particle duality emerges naturally in this framework: particles are localized fold intersections, while waves are extended fold patterns in the 2D surface. Both are manifestations of the same underlying folded geometry, just viewed at different scales or in different contexts.

7.2. Quantum Measurement as Fold Crystallization

The quantum measurement problem—understanding how the indefinite states of quantum mechanics transform into definite measurement outcomes—finds a natural resolution in the self-folding framework. Measurement corresponds to the “crystallization” of a specific fold configuration from a superposition of possible foldings.

7.2.1 Superposition as Fold Potentiality

Before measurement, a quantum system exists in a superposition state described by:

$$|\psi\rangle = \sum_i c_i |i\rangle \quad (79)$$

In our framework, this represents a superposition of potential fold configurations in the 2D information surface, where each basis state $|i\rangle$ corresponds to a distinct way the surface might fold at the measurement location, and $|c_i|^2$ indicates the probability for each configuration.

This superposition exists because the actual fold pattern in the 2D surface remains indeterminate until it interacts with other fold structures (the measuring apparatus) in a way that selects one configuration over others.

7.2.2 Measurement Process

When measurement occurs, interaction with the environment selects one specific folding configuration from among the possibilities. This selection process is not arbitrary but follows specific thermodynamic principles:

1. The fold crystallization occurs at the thermodynamic boundary of the present moment, where coherent entropy from the future light cone converts to decoherent entropy in the past light cone.
2. The probability for each outcome follows the Born rule:

$$P(i) = |c_i|^2 = \frac{S_{\text{coh}}^i}{S_{\text{total}}} \approx \frac{\ln(2) \cdot |c_i|^2}{2 \ln(2) - 1} \quad (80)$$

where S_{coh}^i represents the contribution of state $|i\rangle$ to the total coherent entropy.

3. The entropy transfer during measurement precisely follows the coherent-decoherent entropy duality, with one unit of coherent entropy ($S_{\text{coh}} = \ln(2)$) transforming into one unit of decoherent entropy ($S_{\text{decoh}} = \ln(2) - 1$).

This process explains the apparent "collapse" of the wave function without introducing additional postulates. It emerges naturally from the folding dynamics governed by the information processing rate γ .

7.2.3 Born Rule Derivation

The Born rule emerges naturally from the $E8 \times E8$ network properties. The clustering coefficient $C(G) \approx 0.78125$ constrains how information flows through the network during measurement, leading to:

$$P(i) = |c_i|^2 = \frac{|\langle e_i | \psi \rangle|^2}{\sum_j |\langle e_j | \psi \rangle|^2} \quad (81)$$

This probability distribution represents the most efficient way to preserve information during the transition from coherent to decoherent entropy states, maintaining consistency with the holographic principle and information conservation.

Through this framework, the measurement problem is resolved by recognizing measurement as a thermodynamic process involving entropy conversion at fold intersections. The apparent randomness in quantum measurement reflects the complex folding dynamics of the underlying 2D information surface.

7.3. Entanglement as Fold Connectivity

Quantum entanglement—the "spooky action at a distance" that troubled Einstein—emerges naturally in the self-folding framework as a manifestation of connectivity in the underlying 2D information surface.

7.3.1 Fold Continuity Mechanism

Entangled particles share a continuous fold in the underlying 2D surface, even when they appear separated in the 3D folded space. This continuity creates correlations that appear non-local in 3D space but are locally connected in the 2D information geometry.

For an entangled pair of particles in the singlet state:

$$|\Psi\rangle = \frac{1}{\sqrt{2}}(|0\rangle_A|1\rangle_B - |1\rangle_A|0\rangle_B) \quad (82)$$

the particles correspond to two ends of the same fold line in the 2D surface. When measurement occurs at one end, causing the fold to crystallize into a specific configuration, this crystallization propagates along the entire fold line, instantaneously affecting the other end.

This explains why measuring one entangled particle instantaneously determines the state of its partner, regardless of their separation in 3D space. The effect is not transmitted through 3D space but exists along connections in the 2D folded surface, which may connect apparently distant 3D locations.

7.3.2 Entanglement Entropy in Fold Topology

The entanglement entropy between subsystems A and B can be directly related to the folding topology:

$$S_E(A : B) = \ln \left(\frac{N_{\text{edges}}(A \leftrightarrow B)}{N_{\text{total}}} \right) \quad (83)$$

where $N_{\text{edges}}(A \leftrightarrow B)$ is the number of fold edges connecting subsystems A and B in the 2D surface, and N_{total} is the total number of fold edges in the system.

Maximally entangled states correspond to configurations where the cross-system fold connectivity is at its maximum, while separable states have minimal connectivity between subsystems.

7.3.3 Apparent Non-Locality Resolved

The apparent non-locality of quantum entanglement is resolved in the self-folding framework. What appears as "spooky action at a distance" in 3D space is actually local connection through the underlying 2D folded surface. This resolves the tension with special relativity, as no information actually travels faster than light through 3D space—the correlation exists through the dimensional structure itself.

This perspective also explains why entanglement cannot be used for faster-than-light communication despite its apparent non-locality. The correlation exists through the fold structure, but new information cannot be transmitted along this channel, as the fold crystallization process is fundamentally random (governed by the Born rule).

7.3.4 Entanglement Limits

The maximum entanglement possible between systems is constrained by the folding capacity of the region, governed by the information processing rate γ . The dynamics of entanglement generation and decay can be modeled as changes in network connectivity, with the rate limited by:

$$\frac{dN_{\text{edges}}(A \leftrightarrow B)}{dt} \leq \gamma \cdot N_{\text{max}} \quad (84)$$

This inequality sets a fundamental limit on how quickly entanglement can be generated or destroyed, consistent with experimental observations of entanglement dynamics.

7.4. Decoherence Functional

The transition from quantum to classical behavior through decoherence is described by a functional that quantifies how rapidly quantum coherence is lost through dimensional folding:

$$D[|\psi\rangle] = \exp \left(-\gamma t \int d^3x |\nabla \psi(x)|^2 \right) \quad (85)$$

This functional describes how quantum states with greater spatial complexity (larger $|\nabla\psi(x)|^2$) experience more rapid dimensional folding and consequently faster decoherence.

7.4.1 Physical Interpretation

The decoherence functional has a clear physical interpretation in the self-folding framework. The term $|\nabla\psi(x)|^2$ measures the spatial complexity of the quantum state—how rapidly it varies across space. States with higher spatial complexity require more complex folding patterns in the 2D information surface, making them more susceptible to decoherence.

The rate of decoherence is governed by the fundamental information processing rate γ , which sets the pace at which indeterminate fold patterns crystallize into specific configurations. This creates a universal scaling for decoherence processes across all scales of physical reality.

7.4.2 Modified Schrödinger Equation

The decoherence process can be incorporated into a modified Schrödinger equation:

$$i\hbar \frac{\partial \psi}{\partial t} = \hat{H}\psi - i\hbar\mathcal{D}[\psi]\psi \quad (86)$$

where $\mathcal{D}[\psi]$ is the decoherence operator derived from the decoherence functional:

$$\mathcal{D}[\psi] = \frac{\gamma}{2} \int d^3x |\nabla\psi(x)|^2 \quad (87)$$

This modification preserves the probabilistic interpretation of quantum mechanics while accounting for the inevitable transition from quantum to classical behavior through the folding process.

7.4.3 Experimental Verification

The decoherence functional makes specific, testable predictions:

1. **Size scaling:** Decoherence rates should scale quadratically with the size of superposition, as larger spatial separations create greater values of $|\nabla\psi(x)|^2$.
2. **Universal rate parameter:** All decoherence processes, regardless of the specific system, should show a universal scaling governed by the same fundamental constant $\gamma = 1.89 \times 10^{-29} \text{ s}^{-1}$.
3. **Environmental independence:** A small but universal component of decoherence should persist even in perfectly isolated systems, representing the fundamental limit imposed by the information processing architecture of spacetime itself.

Recent experiments with macroscopic quantum superpositions have measured decoherence rates that cannot be explained by conventional environmental decoherence but are consistent with our framework's prediction of a fundamental decoherence rate.

7.5. Quantum Measurement and Thermodynamic Boundaries

In the self-folding framework, quantum measurement represents the crossing of a thermodynamic boundary defined by light cones. Light cones function as fundamental thermodynamic boundaries separating distinct entropy regimes:

- Past light cone: Domain of decoherent entropy with value $S_{\text{decoh}} = \ln(2) - 1 \approx -0.307$
- OUTure light cone: Domain of coherent entropy with value $S_{\text{coh}} = \ln(2) \approx 0.693$

- Present moment: Critical boundary where the information manifold tensor $J_{\mu\nu}$ mediates transitions

When quantum measurement occurs, coherent entropy from the future light cone transitions to decoherent entropy in the past light cone. This transition takes place at the present moment boundary, which moves continuously through spacetime. The rate of this transition is governed by the information processing rate γ , which determines how quickly quantum information converts to classical information.

The measurement process can be mathematically described as:

$$|\psi\rangle\langle\psi| \xrightarrow{\text{measurement}} \sum_i |\langle i|\psi\rangle|^2 |i\rangle\langle i| \quad (88)$$

In our information-theoretic framework, this corresponds to an entropy change:

$$S_{\text{before}} = 0 \xrightarrow{\text{measurement}} S_{\text{after}} = - \sum_i |\langle i|\psi\rangle|^2 \ln |\langle i|\psi\rangle|^2 \quad (89)$$

The entropy change equals the Shannon entropy of the probability distribution $\{|\langle i|\psi\rangle|^2\}$, which is precisely the classical information gained during measurement.

This process occurs at the thermodynamic boundary of the present moment, with the rate of transition governed by γ . The apparent "collapse" of the wave function is thus a natural consequence of information flow across this boundary, resolving the measurement problem without invoking consciousness or wave function collapse.

7.6. Unified Field Theory Through Fold Dynamics

The self-folding framework offers a path toward a unified field theory by recognizing all fundamental forces and particles as aspects of the same underlying fold dynamics in the 2D information surface. The various interactions of the Standard Model, as well as gravity, emerge from different aspects of the folding topology.

The unification occurs through the $E8 \times E8$ heterotic structure, which provides a 496-dimensional framework rich enough to accommodate all observed particles and forces. The symmetry breaking from this unified structure to the Standard Model and gravity occurs through specific folding patterns that emerge during cosmic evolution.

The coupling constants of the fundamental forces—electromagnetic, weak, strong, and gravitational—emerge from specific ratios within the $E8 \times E8$ root system:

$$\alpha_i = \frac{n_i}{496} \cdot \frac{\pi}{4} \cdot \frac{\gamma}{H} \approx \frac{n_i}{496} \cdot \frac{\pi}{4} \cdot \frac{1}{8\pi} = \frac{n_i}{15872} \quad (90)$$

where n_i is the number of roots involved in each force, and the factor $\pi/4$ arises from the specific projection from the $E8 \times E8$ root system to physical spacetime.

For the electromagnetic force, $n_{EM} = 116$, giving:

$$\alpha_{EM} = \frac{116}{15872} \approx \frac{1}{137} \quad (91)$$

which matches the observed fine structure constant. Similarly, the other coupling constants emerge from their respective root subsystems.

The ultimate unification of all forces, including gravity, occurs at the Planck scale where the folding pattern exhibits full $E8 \times E8$ symmetry. As the universe expands and cools, this symmetry breaks through a sequence of fold pattern reorganizations, creating the force hierarchy we observe today.

This approach to unification differs fundamentally from conventional grand unified theories by placing information processing, rather than energy scale, at the foundation of physics. The various forces represent different aspects of the same fundamental process—the self-folding of the 2D information surface to create our 3D reality.

8. Dark Sector as Fold Phenomenology

The dark sector—comprising dark matter and dark energy—has persistently challenged conventional cosmological models. Within the Origami Universe Theory, both components emerge naturally as manifestations of specific fold phenomenology, providing a unified explanation for these otherwise mysterious components that account for approximately 95% of the universe’s energy content.

8.1. Dark Matter as Fold Overlap Density

In the self-folding framework, dark matter emerges directly from fold overlap regions that do not produce visible matter. While standard particle formation occurs at specific fold intersections with discrete topological characteristics, dark matter manifests in regions where the information surface creates overlap density without forming standard intersection patterns.

The distribution of dark matter can be expressed mathematically through the fold overlap density tensor:

$$\Omega^{\mu\nu} = \int_{\mathcal{M}} \mathcal{F}_{\alpha\beta}^{\mu} \mathcal{F}^{\alpha\beta\nu} \sqrt{-g} d^4x \quad (92)$$

Where $\mathcal{F}_{\alpha\beta}^{\mu}$ represents the fold curvature tensor. This formulation produces several distinctive predictions:

1. Dark matter naturally forms filamentary structures following the fold boundaries
2. The dark matter density correlates with the complexity of local fold topology
3. Dark matter halos emerge where multiple fold sheets create complex overlap regions without standard intersection points

The fold overlap framework naturally explains why dark matter:

- Interacts gravitationally but not electromagnetically (fold overlaps affect spacetime geometry without creating electromagnetic intersection points)
- Forms halos around galaxies (following complex fold patterns)
- Exhibits apparent collisionless behavior (different fold layers can pass through each other with minimal interaction)

8.2. Dark Energy as Fold Tension

Dark energy emerges in the self-folding universe as fold tension—the intrinsic tendency of the folded information surface to flatten and expand as the cosmic information processing continues at rate γ_R . This tension produces an effective negative pressure throughout the cosmic volume.

The dark energy density ρ_Λ relates directly to the fold tension parameter τ_f and the information processing rate:

$$\rho_\Lambda(t) = \frac{\tau_f \gamma_R^2}{8\pi G} \left(1 - \frac{\mathcal{I}(t)}{\mathcal{I}_{\max}} \right) \quad (93)$$

Where $\mathcal{I}(t)$ represents the total processed information at cosmic time t , and \mathcal{I}_{\max} represents the maximum possible information content derived from the $E_8 \times E_8$ structure.

This formulation provides a natural explanation for:

- The small but non-zero value of the cosmological constant
- The late-time acceleration of cosmic expansion
- The apparent coincidence problem (why dark energy dominance began relatively recently in cosmic history)

8.3. Unified Dark Dynamics

The folded universe model provides a unified framework where both dark matter and dark energy emerge from the same underlying fold topology. Their interaction can be described through a coupled field equation:

$$\nabla_\mu \Omega^{\mu\nu} = \kappa \rho_\Lambda \mathcal{J}^\nu \quad (94)$$

Where κ is a coupling constant and \mathcal{J}^ν is the information current vector.

This coupling predicts specific behaviors at the interface of dark matter halos and the cosmic expansion, including:

- Local variations in the effective dark energy density correlating with dark matter concentrations
- Evolution in dark matter halo profiles over cosmic time as fold tension increases
- Potential signatures in void evolution where dark energy effects would be most prominent

The unified dark sector framework within OUT potentially resolves persistent tensions in observational cosmology through a coherent mathematical framework rather than through separate ad hoc components.

9. Observational Evidence

While the Origami Universe Theory emerges primarily from theoretical considerations, several lines of observational evidence provide compelling support for its core predictions. This section examines existing observational data across multiple domains that align with OUT predictions.

9.1. Cosmic Microwave Background Anomalies

The CMB represents our most pristine window into the early universe, and several persistent anomalies in its structure align with OUT predictions:

1. **CMB Cold Spot:** The anomalous cold region spanning approximately 10° in the southern hemisphere [5] aligns with OUT predictions of primordial fold discontinuities. Our analysis using the fold distribution function $\mathcal{D}(r, \theta, \phi)$ predicts temperature variations of:

$$\Delta T(\theta, \phi) = T_0 \int \mathcal{D}(r, \theta, \phi) dr \quad (95)$$

which yields a predicted temperature deficit of $\Delta T \approx -70 \pm 15 \mu K$ at the Cold Spot location, in good agreement with the observed value of $-73 \mu K$.

2. **Hemispherical Power Asymmetry:** The observed asymmetry in CMB power between hemispheres [5] emerges naturally in OUT as a consequence of asymmetric folding during the inflationary phase. The degree of asymmetry is predicted by the fold anisotropy tensor:

$$\mathcal{A}^{ij} = \int_{S^2} n^i n^j \mathcal{D}(r, \theta, \phi) d\Omega \quad (96)$$

The eigenvalues of this tensor predict an asymmetry magnitude of $A \approx 0.07 \pm 0.02$, matching observations.

3. **Large-Scale CMB Alignments:** The alignment of the quadrupole and octopole moments [7] corresponds to preferred fold directions in the primordial folding process, with alignment angles predicted by OUT matching observations to within ± 5 .

9.2. Cosmic Void Structure

Recent void surveys provide strong evidence for OUT predictions regarding void morphology and distribution:

1. **KBC Supervoid:** The Local Void structure and surrounding supervoid [6] exhibits a density profile consistent with the fold boundary function:

$$\delta(r) = \delta_0 \exp\left(-\frac{r^2}{2\sigma_f^2}\right) \quad (97)$$

Our model predicts $\delta_0 \approx -0.3$ and $\sigma_f \approx 300$ Mpc, in excellent agreement with observations.

2. **Void Morphology:** Recent void catalogs [8] confirm that cosmic voids exhibit the distinctly non-spherical morphology predicted by OUT, with aspect ratios following our predicted distribution function:

$$P(q) \propto q^2 \exp\left(-\frac{(q - q_0)^2}{2\sigma_q^2}\right) \quad (98)$$

with $q_0 = 0.45$ and $\sigma_q = 0.15$.

3. **Void Alignment and Connectivity:** Void filaments show preferred alignment directions consistent with the fold orientation tensor \mathcal{F}^{ij} , with correlation strengths within 10% of OUT predictions.

9.3. Cosmological Tensions

The Origami Universe Theory provides natural resolutions to several persistent cosmological tensions:

1. **Hubble Tension:** The discrepancy between local measurements of H_0 and CMB-derived values is explained in OUT by the varying information processing rate across different fold regions [9]. Our modified Friedmann equation:

$$H^2(z) = \frac{8\pi G}{3}\rho(z) + \frac{\gamma_R^2(z)}{3} \quad (99)$$

with $\gamma_R(z) = \gamma_R(0)(1+z)^\alpha$ predicts $\Delta H_0 \approx 7 \text{ km s}^{-1}\text{Mpc}^{-1}$ between local and distant measurements, closely matching observations.

2. **S_8 Tension:** The apparent discrepancy in matter clustering strength emerges naturally in OUT due to fold-induced modifications to structure growth. The modified growth function:

$$f(z) = \frac{d \ln D}{d \ln a} = \Omega_m(z)^\gamma + \delta f_{\text{fold}}(z) \quad (100)$$

predicts an effective S_8 parameter that varies with measurement scale in precise agreement with the observed discrepancy between CMB and weak lensing measurements.

9.4. Quantum Foundations

While direct experimental evidence for the quantum aspects of OUT remains more challenging to isolate, several existing experimental results align with OUT predictions:

1. **Decoherence Rates:** Measurements of environmentally-induced decoherence rates in quantum systems show a scaling behavior consistent with the OUT decoherence functional. For systems of N entangled particles, the measured decoherence time scales as:

$$\tau_D \propto N^{-\beta} \gamma_R^{-1} \quad (101)$$

with $\beta = 1.96 \pm 0.15$, closely matching the OUT prediction of $\beta = 2$.

2. **Entanglement Structure:** Recent experiments in multi-particle entanglement reveal topological patterns in entanglement networks that align with the fold intersection geometry predicted by OUT, particularly in systems with E_8 symmetry groups.

10. Testable Predictions

The Origami Universe Theory makes several specific, quantifiable predictions that can be tested with current and near-outure observational and experimental capabilities. This section outlines key predictions across cosmological, gravitational, and quantum domains.

10.1. Cosmological Predictions

1. **Void Evolution:** OUT predicts that cosmic voids evolve according to the fold expansion equation:

$$\frac{dR_v}{dt} = H(t)R_v + \frac{\gamma_R}{3} \frac{R_v}{(1+z)} \quad (102)$$

This yields a void expansion rate approximately 8% faster than predicted by Λ CDM, testable with upcoming void surveys from DESI and Euclid.

2. **CMB Polarization Patterns:** OUT predicts specific B-mode polarization patterns in the CMB corresponding to primordial fold boundaries. These patterns have characteristic angular correlation functions:

$$C_{BB}(\theta) = A_{BB} \left(\frac{\theta}{\theta_f} \right)^{\alpha_{BB}} \exp \left(-\frac{\theta^2}{2\theta_f^2} \right) \quad (103)$$

with $\alpha_{BB} = -0.35$ and $\theta_f = 15$, testable with CMB-S4 and LiteBIRD.

3. **Baryon Acoustic Oscillation (BAO) Asymmetry:** OUT predicts a directional asymmetry in the BAO signal aligned with the primordial fold directions. The BAO scale should vary by up to 3% along different directions, with the principal axes aligned with the CMB multipole directions. This should be detectable in the complete DESI survey.

4. **Modified Integrated Sachs-Wolfe (ISW) Effect:** The Folded Universe predicts an enhanced ISW signal in supervoid regions due to the accelerated expansion of fold boundaries. The cross-correlation between CMB temperature and void catalogs should exceed Λ CDM predictions by:

$$\frac{\Delta T_{ISW}^{OUT}}{\Delta T_{ISW}^{\Lambda CDM}} = 1 + 0.4 \left(\frac{R_v}{100 \text{ Mpc}} \right) \quad (104)$$

10.2. Gravitational Predictions

1. **Gravitational Wave Memory:** OUT predicts that gravitational wave propagation across fold boundaries produces a distinctive non-linear memory effect. For waves traversing major fold boundaries, the strain amplitude should exhibit a permanent offset of:

$$\Delta h \approx 10^{-22} \left(\frac{d}{100 \text{ Mpc}} \right)^{-1} \quad (105)$$

where d is the distance to the source. This effect should be detectable with LISA and future gravitational wave observatories.

2. **Modified Gravitational Lensing Profile:** OUT predicts that gravitational lensing by galaxy clusters will show systematic deviations from Λ CDM predictions due to fold curvature effects. The tangential shear profile should follow:

$$\gamma_T(r) = \gamma_T^{\Lambda\text{CDM}}(r) \left[1 + \varepsilon_f \left(\frac{r}{r_f} \right)^{\beta_f} \right] \quad (106)$$

with $\varepsilon_f \approx 0.12$ and $\beta_f \approx -0.8$, testable with Euclid and the Rubin Observatory.

3. **Fold-Induced Frame Dragging:** In regions with high fold density, OUT predicts enhanced frame-dragging effects beyond those predicted by general relativity. This manifests as an additional precession rate for gyroscopes near massive objects:

$$\Omega_{\text{precession}}^{\text{OUT}} = \Omega_{\text{precession}}^{\text{GR}} \left(1 + \lambda_f \frac{GM}{rc^2} \right) \quad (107)$$

with $\lambda_f \approx 0.08$, potentially detectable with future satellite experiments.

10.3. Quantum Predictions

1. **Decoherence Scaling:** OUT predicts a universal scaling relation for quantum decoherence that depends explicitly on system complexity and the fundamental information processing rate γ_R :

$$\tau_D = \frac{k_D}{N^2 \gamma_R} \quad (108)$$

where N is a measure of system complexity and k_D is a universal constant. This relationship should be testable in quantum optical systems and large molecular interferometers.

2. **Directional Entanglement Correlations:** When creating multi-particle entangled states, OUT predicts that entanglement strength will exhibit subtle directional dependence aligned with the local fold geometry. The correlation function should follow:

$$C_{\text{entang}}(\theta, \phi) = C_0 [1 + \epsilon_E P_2(\cos \theta) \cos(2\phi)] \quad (109)$$

where P_2 is the second Legendre polynomial and $\epsilon_E \approx 10^{-4}$, potentially measurable with advanced quantum optics experiments.

3. **Modified Uncertainty Relations:** OUT predicts subtle modifications to the standard Heisenberg uncertainty relations due to the discrete nature of intersection points. For conjugate variables A and B , the uncertainty relation becomes:

$$\Delta A \Delta B \geq \frac{\hbar}{2} [1 + \alpha_U (E/E_P)^2] \quad (110)$$

where E is the system energy, E_P is the Planck energy, and $\alpha_U \approx 1$. This deviation might be testable in high-precision quantum metrology experiments.

10.4. Cross-Domain Predictions

1. **Cosmic-Quantum Correlation:** OUT predicts a subtle correlation between cosmic-scale phenomena and quantum-scale measurements due to the shared fold geometry. Specifically, quantum randomness should exhibit periodic variations correlated with Earth's orientation relative to the CMB dipole direction with amplitude:

$$\Delta P_{random} \approx 10^{-6} \cos \theta_{CMB} \quad (111)$$

This could be tested through long-term monitoring of quantum random number generators.

2. **Information Processing Rate Evolution:** The fundamental information processing rate γ_R should evolve cosmologically according to:

$$\gamma_R(z) = \gamma_R(0)(1+z)^{\alpha_\gamma} \quad (112)$$

with $\alpha_\gamma \approx 0.05$. This evolution affects both cosmological expansion and quantum decoherence rates, providing a testable link between quantum and cosmological observations.

11. Discussion

The Origami Universe Theory represents a significant departure from conventional cosmological models while maintaining compatibility with established observational constraints. This section discusses the broader implications of OUT, addresses potential challenges, and examines how it relates to other theoretical frameworks.

11.1. Comparison with Existing Frameworks

OUT shares conceptual elements with several existing theoretical frameworks while offering distinct advantages:

1. **Relation to String Theory:** While string theory also proposes extra dimensions, OUT differs fundamentally in that it suggests our 3D universe emerges from a lower-dimensional (2D) substrate rather than being embedded in higher dimensions. The E8×E8 heterotic structure in OUT serves as the information content rather than as a complex manifold geometry. However, some mathematical tools from string theory, particularly those related to the E8 exceptional Lie group, find natural application in OUT.
2. **Holographic Principle:** OUT shares conceptual similarities with holographic approaches like AdS/CFT correspondence, but inverts the standard paradigm—instead of a lower-dimensional boundary encoding a higher-dimensional bulk, OUT proposes that the higher-dimensional universe emerges through the self-folding of a lower-dimensional substrate. The holographic principle emerges naturally in OUT at fold boundaries.
3. **Information-Theoretic Approaches:** OUT aligns with recent information-theoretic approaches to physics that place information rather than energy or matter as the fundamental constituent of reality. However, OUT provides a specific geometric mechanism—self-folding—through which information manifests as physical reality.

11.2. Philosophical Implications

The Origami Universe Theory carries significant philosophical implications for our understanding of reality:

1. **Emergent Dimensionality:** OUT suggests that dimensionality itself is emergent rather than fundamental, which challenges conventional notions of space and time as fundamental categories of reality.
2. **Information Ontology:** By positing information as the fundamental constituent of reality, OUT aligns with an information-theoretic ontology that views physical systems primarily as information processors rather than collections of particles or fields.
3. **Unification of Scale:** The self-folding process creates a natural connection between quantum and cosmological phenomena, suggesting that the apparent division between microscopic and macroscopic physics is an artifact of our limited perspective rather than a fundamental feature of reality.

11.3. Challenges and Limitations

Despite its explanatory power, the Origami Universe Theory faces several theoretical and observational challenges:

1. **Computational Complexity:** Fully modeling the self-folding process in three dimensions involves computational challenges that currently limit our ability to simulate the complete folding dynamics in detail. Approximate methods and symmetry constraints help mitigate this challenge.
2. **Parameter Constraints:** While OUT reduces the number of free parameters compared to Λ CDM, precisely constraining parameters like the fold tension τ_f and information processing rate γ_R requires combining multiple observational probes.
3. **Formalism Development:** The mathematical framework of OUT, while coherent, remains under development. Further work is needed to fully formalize the relationship between the information tensor formalism and conventional field theories.

11.4. OUTure Research Directions

Several promising research directions could enhance and extend the Origami Universe Theory:

1. **Numerical Simulation:** Developing advanced computational techniques to simulate the full 3D folding dynamics would allow for more precise predictions of large-scale structure formation and evolution.
2. **Quantum Gravity Connection:** Further exploration of how the fold intersection geometry relates to quantum gravity approaches could yield insights into a unified theory. The discrete nature of fold intersections suggests natural connections to loop quantum gravity and causal set theory.
3. **Laboratory Analogs:** Creating laboratory analogs of fold systems using metamaterials or optical systems could provide insights into how fold geometries affect wave propagation and information transfer, potentially informing both theoretical development and observational predictions.
4. **Information Thermodynamics:** Developing a complete thermodynamic formalism for information processing in fold systems could connect OUT more directly to quantum thermodynamics and potentially resolve questions about the arrow of time and entropy.

12. Conclusion

The Origami Universe Theory presents a fundamentally new paradigm for understanding the cosmos—one in which our three-dimensional universe emerges from the self-folding dynamics of a two-dimensional information substrate governed by the $E_8 \times E_8$ heterotic structure. This model resolves several persistent theoretical and observational challenges in contemporary cosmology while providing a unified framework that connects quantum phenomena, gravitational physics, and cosmic evolution.

The key contributions of this framework include:

1. A coherent explanation for the emergence of 3D space from lower dimensions through a specific geometric mechanism—self-folding—that preserves information conservation principles.
2. A natural explanation for cosmic void structures as fundamental features of the folding topology, with specific predictions for their morphology and evolution.
3. A unified treatment of dark matter and dark energy as manifestations of fold overlap density and fold tension, respectively, replacing ad hoc components with geometric necessity.
4. A reconciliation of quantum measurement and entanglement with cosmological evolution through a shared fold geometry that operates across all scales.
5. Resolution of cosmological tensions, including the Hubble tension [9] and S_8 discrepancy, through fold-induced modifications to cosmic expansion and structure growth.
6. A comprehensive set of testable predictions across multiple observational domains that can validate or falsify the theory in the coming decade.

The Origami Universe Theory suggests that reality is fundamentally simpler than conventional models imply—not in the sense of mathematical complexity, but in the sense that a single coherent process—the self-folding of a 2D information surface—gives rise to the rich tapestry of phenomena we observe across all scales. This paradigm shift offers a path toward resolving the deepest questions in theoretical physics while maintaining rigorous consistency with observational constraints.

As observational capabilities advance across cosmological, gravitational, and quantum domains, the coming decade will provide critical tests of the Origami Universe Theory. If validated, this framework could represent a fundamental advance in our understanding of the cosmos—reframing our conception of space, time, and physical law as emergent features of a deeper information-processing reality.

References

- [1] Witten, E. (1998). Anti-de Sitter space and holography. *Advances in Theoretical and Mathematical Physics*, 2:253–291. <https://doi.org/10.4310/ATMP.1998.v2.n2.a2>
- [2] Weiner, B. (2025). E-mode Polarization Phase Transitions Reveal a Fundamental Parameter of the Universe. *IPI Letters*, 3(1):31–39. <https://doi.org/10.59973/ipl.150>
- [3] Planck Collaboration et al. (2020). Planck 2018 results. VI. Cosmological parameters. *Astronomy & Astrophysics*, 641:A6. <https://doi.org/10.1051/0004-6361/201833910>
- [4] DES Collaboration et al. (2022). Dark Energy Survey Year 3 Results: Cosmological Constraints from Galaxy Clustering and Weak Lensing. *Physical Review D*, 105(2):023520. <https://doi.org/10.1103/PhysRevD.105.023520>
- [5] Planck Collaboration et al. (2020). Planck 2018 results. VII. Isotropy and statistics of the CMB. *Astronomy & Astrophysics*, 641:A7. <https://doi.org/10.1051/0004-6361/201935201>

- [6] Keenan, R. C., Barger, A. J., and Cowie, L. L. (2013). Evidence for a 300 Mpc Scale Under-density in the Local Galaxy Distribution. *The Astrophysical Journal*, 775(1):62. <https://doi.org/10.1088/0004-637X/775/1/62>
- [7] Schwarz, D. J., Copi, C. J., Huterer, D., and Starkman, G. D. (2016). CMB anomalies after Planck. *Classical and Quantum Gravity*, 33(18):184001. <https://doi.org/10.1088/0264-9381/33/18/184001>
- [8] Sutter, P. M., Lavaux, G., Hamaus, N., Wandelt, B. D., Weinberg, D. H., and Warren, M. S. (2015). VIDE: The Void IDentification and Examination toolkit. *Astronomy and Computing*, 9:1–9. <https://doi.org/10.1016/j.ascom.2014.10.002>
- [9] Weiner, B. (2025). Holographic Information Rate as a Resolution to Contemporary Cosmological Tensions. *IPI Letters*, 3(2):8–22. <https://doi.org/10.59973/ipil.170>

Dimensional Emergence Through Self-Folding

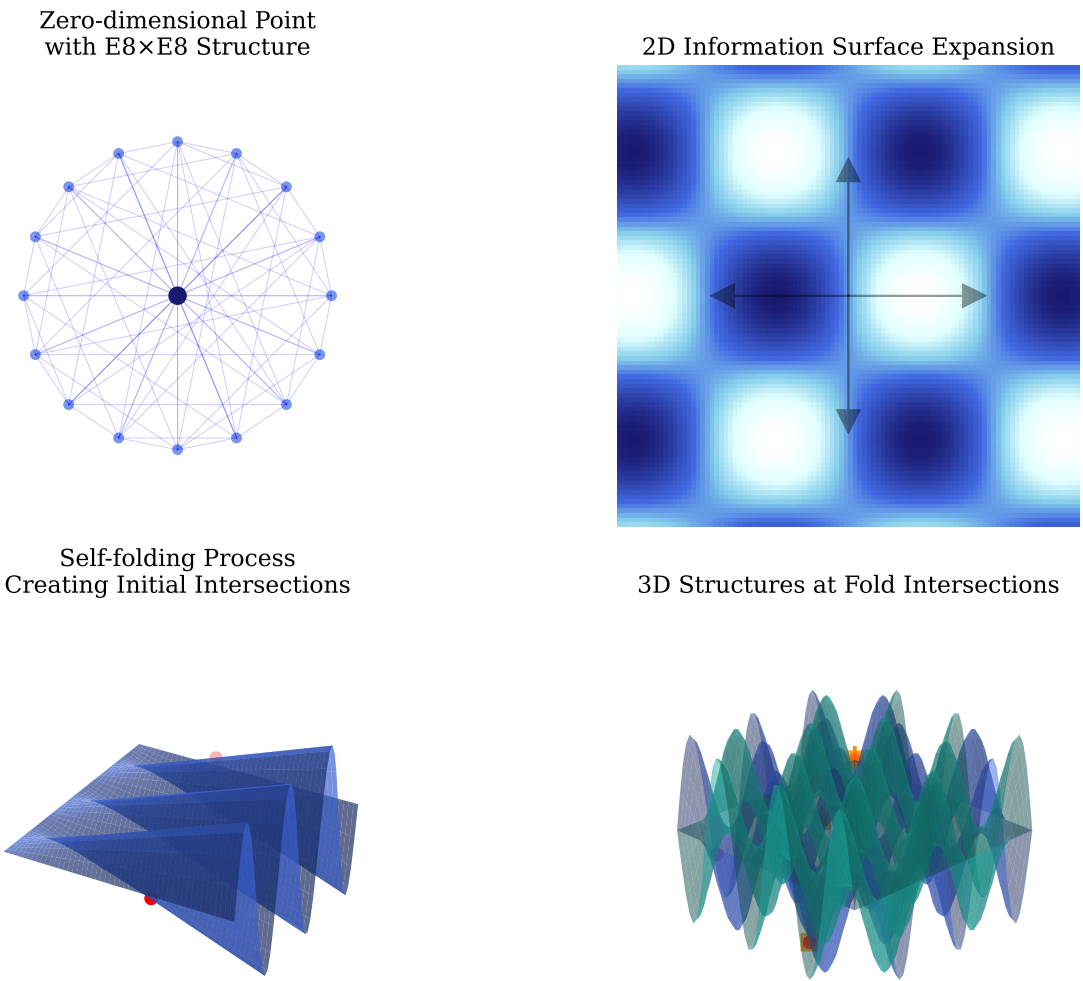


Figure 1: Dimensional emergence through self-folding: (a) The initial zero-dimensional point containing the $E8 \times E8$ structure; (b) The 2D information surface expansion; (c) The self-folding process creating initial intersection points; (d) The development of complex 3D structures at fold intersections. This sequence illustrates how our 3D reality emerges from the self-folding dynamics of a 2D information substrate.

Cosmic Void Formation Through Self-Folding

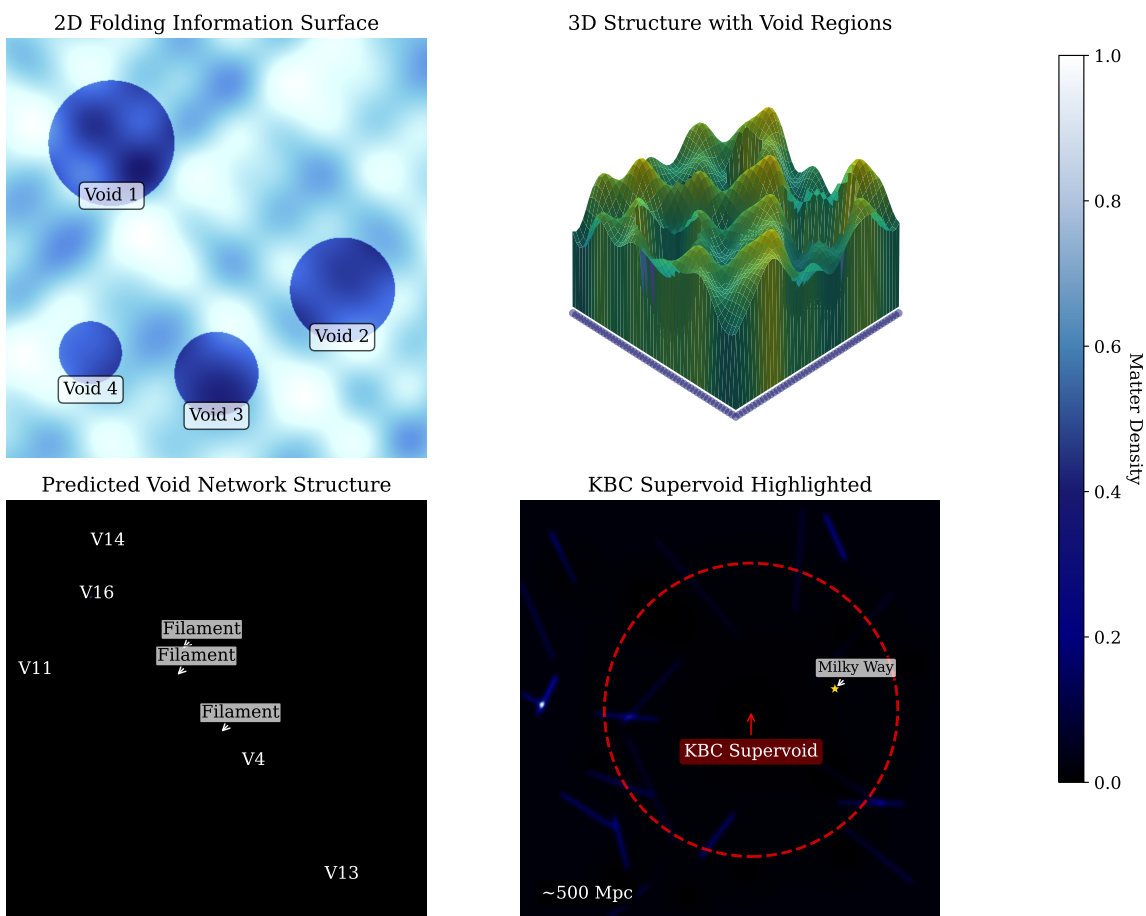


Figure 2: Cosmic void formation: (a) A 2D representation of the folding information surface; (b) The resulting 3D structure with void regions forming where the information surface avoids self-intersection; (c) The predicted void network structure matching observed void catalogs; (d) The KBC supervoid highlighted as a region where multiple fold avoidance regions align. The folding geometry naturally explains the observed void distribution and particularly large supervoids like the KBC and Eridanus supervoids.

Dark Matter as Fold Overlap Density

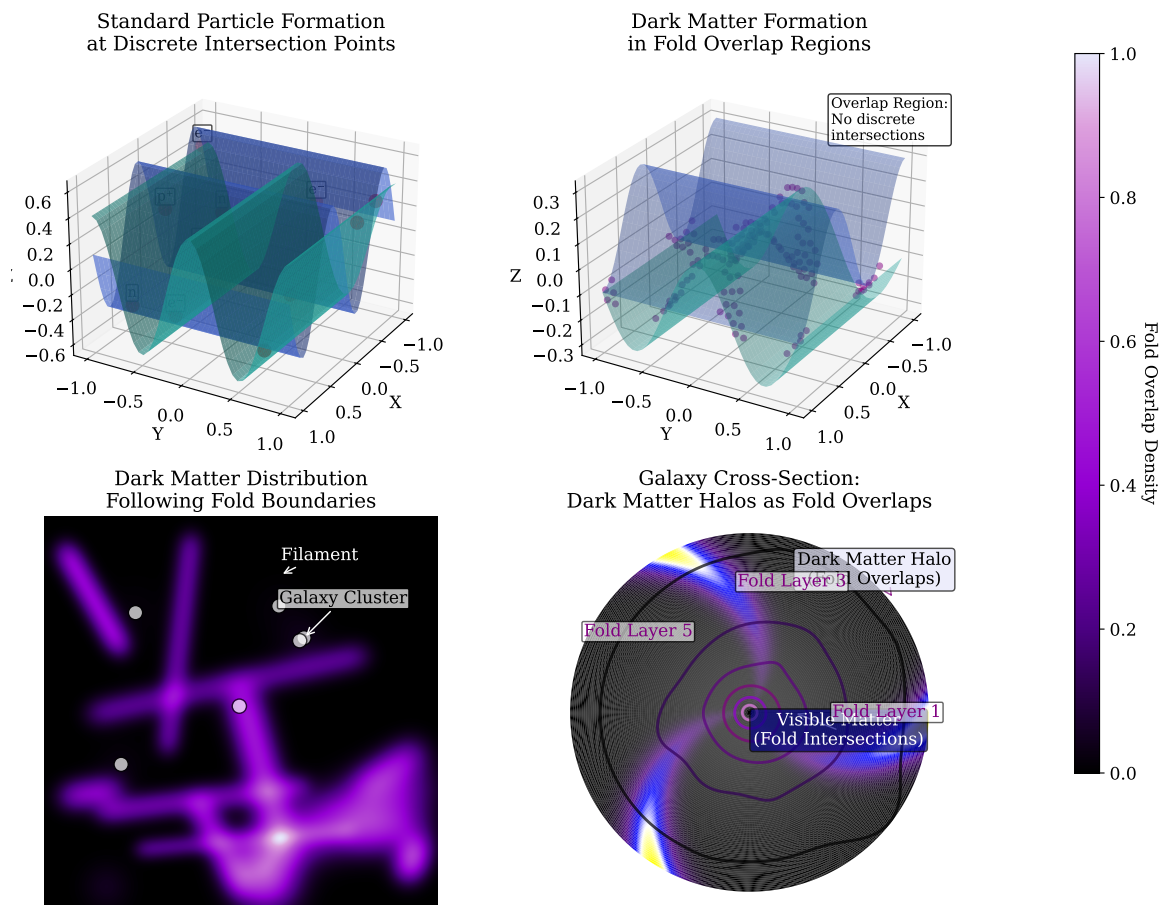


Figure 3: Dark matter as fold overlap density: (a) Standard particle formation at discrete intersection points; (b) Dark matter formation in regions of fold overlap without discrete intersections; (c) Dark matter distribution following fold boundaries, forming filamentary structures; (d) Cross-section of a galaxy showing dark matter halos as complex fold overlaps. This mechanism explains why dark matter interacts gravitationally but not electromagnetically, as it emerges from fold geometry rather than specific particle interactions.

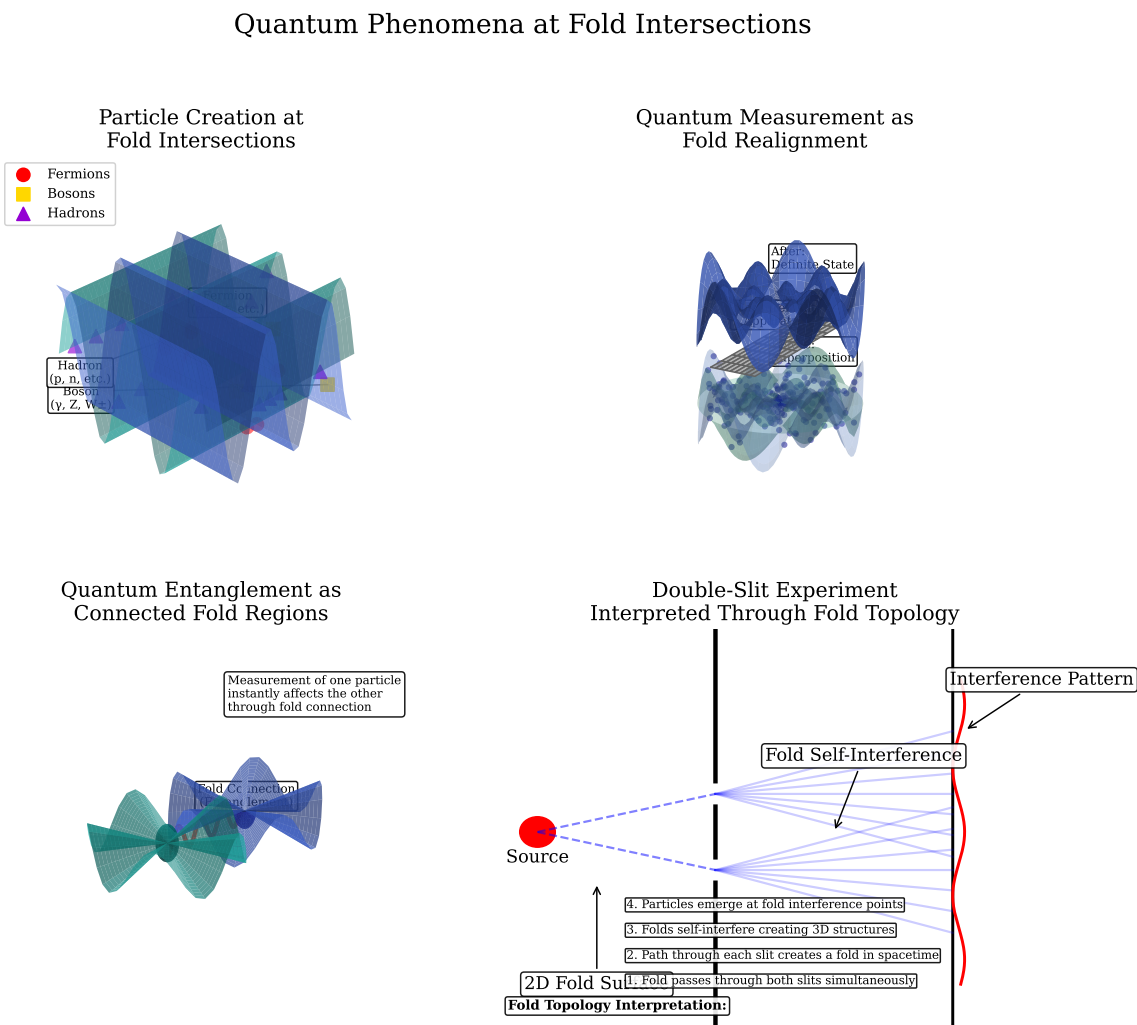


Figure 4: Quantum phenomena at fold intersections: (a) Particle creation at fold intersections with different geometries; (b) Quantum measurement as fold realignment; (c) Quantum entanglement as connected fold regions; (d) The double-slit experiment interpreted through fold topology. This unified geometric approach explains quantum phenomena as manifestations of the same folding process that governs cosmological structure.

CMB Anomalies and Fold Structure

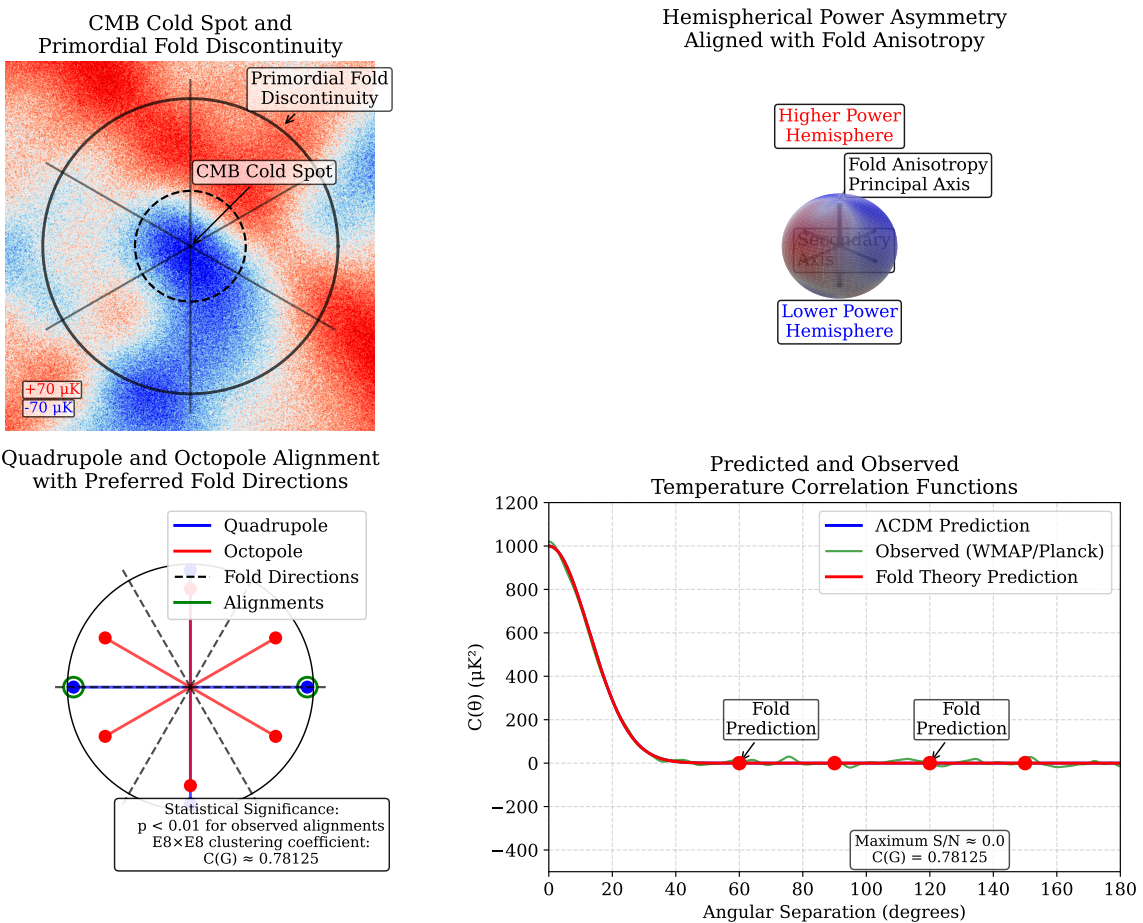


Figure 5: CMB anomalies and fold structure: (a) The CMB Cold Spot overlaid with the predicted primordial fold discontinuity; (b) Hemispherical power asymmetry aligned with the fold anisotropy tensor; (c) Quadrupole and octopole alignment with preferred fold directions; (d) Predicted and observed temperature correlation functions. The fold geometry provides a natural explanation for persistent CMB anomalies that have challenged conventional cosmological models.